

Parameter Sensitivity Analysis of the SparTen High Performance Sparse Tensor Decomposition Software: Extended Analysis

Jeremy M. Myers
Daniel M. Dunlavy
Keita Teranishi
D. S. Hollman

JERMYER@SANDIA.GOV, JMMYERS01@EMAIL.WM.EDU
 DMDUNLA@SANDIA.GOV
 KNTERAN@SANDIA.GOV
 DSHOLLM@SANDIA.GOV

Sandia National Laboratories, Albuquerque, NM 87123, USA
College of William and Mary, Williamsburg, VA 23185, USA

Abstract

Tensor decomposition models play an increasingly important role in modern data science applications. One problem of particular interest is fitting a low-rank Canonical Polyadic (CP) tensor decomposition model when the tensor has sparse structure and the tensor elements are nonnegative count data. SparTen is a high-performance C++ library which computes a low-rank decomposition using different solvers: a first-order quasi-Newton or a second-order damped Newton method, along with the appropriate choice of runtime parameters. Since default parameters in SparTen are tuned to experimental results in prior published work on a single real-world dataset conducted using MATLAB implementations of these methods, it remains unclear if the parameter defaults in SparTen are appropriate for general tensor data. Furthermore, it is unknown how sensitive algorithm convergence is to changes in the input parameter values. This report addresses these unresolved issues with large-scale experimentation on three benchmark tensor data sets. Experiments were conducted on several different CPU architectures and replicated with many initial states to establish generalized profiles of algorithm convergence behavior.

Keywords: tensor decomposition, Poisson factorization, Kokkos, Newton optimization



Sandia National Laboratories is a multimission laboratory managed and operated by National Technology & Engineering Solutions of Sandia, LLC, a wholly owned subsidiary of Honeywell International Inc., for the U.S. Department of Energy's National Nuclear Security Administration under contract DE-NA0003525. SAND2020-11901R



Acknowledgment

We would like to thank Richard Barrett for assistance utilizing computing resources at Sandia National Laboratories and Rich Lehoucq for comments of support.

Contents

1	Introduction	4
2	Background	5
3	Methods	6
3.1	Hardware Platforms	6
3.2	Data	6
3.3	Software Parameter Definitions & Experimental Ranges	7
3.4	Experiments	8
4	Results	10
4.1	General Convergence Results on Real-World Data	11
4.2	Sensitivity of Convergence and Solution Behavior	12
4.2.1	CP-APR	13
4.2.2	Line search	13
4.2.3	Damped Newton (PDNR)	14
4.2.4	Quasi-Newton (PQNR)	16
4.2.5	Numerical stability	16
5	Conclusions	18
	References	19
A	Detailed Experiment Results	20
A.1	Heatmaps	20
A.2	Average Convergence Results	30
List of Figures		
1	Example heatmap illustrating results.	11
3	PDNR, <code>mu_initial</code> . Mean function evaluations and 95% CI. PDNR damps out Hessian information and is more prone to time-outs when <code>mu_initial</code> is large (PDNR, <i>lbnl</i>).	15
4	Mean objective function values with 95% confidence interval, varying <code>eps_div_zero_grad</code> (PDNR, <i>lbnl</i>).	17
5	Experiment outcomes for <i>chicago-crime-comm</i> data on Intel platform.	21
6	Experiment outcomes for <i>lbnl-network</i> data on Intel platform.	22
7	Experiment outcomes for <i>nell-2</i> data on Intel platform.	23
8	Experiment outcomes for <i>chicago-crime-comm</i> data on ARM platform.	24
9	Experiment outcomes for <i>lbnl-network</i> data on ARM platform.	25

10	Experiment outcomes for <i>nell-2</i> data on ARM platform.	26
11	Experiment outcomes for <i>chicago-crime-comm</i> data on IBM platform.	27
12	Experiment outcomes for <i>lbnl-network</i> data on IBM platform.	28
13	Experiment outcomes for <i>nell-2</i> data on IBM platform.	29

List of Tables

1	Hardware characteristics and software environment of the clusters in this paper. <i>Threads</i> and <i>RAM (GB)</i> are per node.	6
2	Sparse tensor datasets from the FROSTT collection.	7
3	SparTen software parameter descriptions and values used in our experiments.	9
4	Experiments run on the different datasets and hardware platforms.	10
5	Average convergence behavior for the <i>chicago-crime-comm</i> data set. Confidence intervals are percentages of the mean.	31
6	Average convergence behavior for the <i>lbnl-network</i> data set. Confidence intervals are percentages of the mean.	32
7	Average convergence behavior for the <i>nell-2</i> data set. Confidence intervals are percentages of the mean.	33

1. Introduction

The Canonical Polyadic (CP) tensor decomposition model has garnered attention as a tool for extracting useful information from high dimensional data across a wide range of applications [9, 3, 8, 2, 7].

Recently, Hansen *et al.* developed two highly-parallelizable Newton-based methods for low-rank tensor factorizations on Poisson count data in [6], one a first-order quasi-Newton method (PQNR) and another a second-order damped Newton method (PDNR). They were first implemented in MATLAB Tensor Toolbox [1] as the function `cp_apr`, referring to this approach as computing a CP decomposition using Alternating Poisson Regression (i.e., CP-APR). These methods fit a reduced-rank CP model to count data, assuming a Poisson error distribution. PDNR and PQNR are implemented in SparTen,¹ a high-performance C++ library of CP-APR solvers for sparse tensors. SparTen improves on the MATLAB implementation to provide efficient execution for large, sparse tensor decompositions, exploiting the Kokkos hardware abstraction library [5] to harness parallelism on diverse HPC platforms, including x86-multicore, ARM, and GPU computer architectures.

SparTen contains many algorithmic parameters for controlling the optimization subroutines comprising PDNR and PQNR. To date, only anecdotal evidence exists for how best to tune the algorithms. Parameter defaults in SparTen were chosen according to previous results using the MATLAB implementations described by Hansen *et al.* [6]. However, their analysis was limited to a single real-world dataset, and thus may not be optimal for computing decompositions of more general tensor data. Furthermore, it is unknown how the initial guess to a solution affects convergence, since SparTen methods may converge slowly—or worse, stagnate—on real data if the initial state is far from a solution. And, lastly, the average impact of input parameters on algorithm convergence is unclear.

To address these unknowns, we present the results of numerical experiments to assess the sensitivity of software parameters on algorithm convergence for a range of values with benchmark tensor problems. Every experiment was replicated with 30 randomly chosen initial guesses on three diverse computer architectures to aid statistical interpretation. With our results, we (1) provide new results that offer a realistic picture of algorithm convergence under reasonable resource constraints, (2) establish practical bounds on parameters such that, if set at or beyond these values, convergence is unlikely, and (3) identify areas of performance degradation and convergence toward qualitatively different results owing to parameter sensitivities.

We limited our study to multicore CPU architectures only, using OpenMP [4] to manage the parallel computations across threads/cores. Although SparTen, through Kokkos, can leverage other execution backends—e.g., NVIDIA’s CUDA framework for GPU computation—we focus solely on diversity in CPU architectures in this work.

This paper is structured as follows. Section 2 summarizes basic tensor notation and details. Section 3 describes the hardware environment, test data, and experimental design of the sensitivity analysis. Section 4 provides detailed results of the sensitivity analyses. Section 5 offers concluding remarks and lays out future work.

1. SparTen is a portmanteau word derived from *Sparse* and *Tensor*. The SparTen code is available at <http://gitlab.com/tensors/sparten>.

2. Background

We briefly describe below the problem we are addressing in this report; for a detailed description of CP decomposition algorithms implemented in SparTen, refer to the descriptions in Hansen *et al.* [6].

An N -way data tensor \mathcal{X} has dimension sizes $I_1 \times I_2 \times \dots \times I_N$. We wish to fit a reduced-dimension tensor model, \mathcal{M} , to \mathcal{X} . The R -component Canonical Polyadic (CP) decomposition is given as follows:

$$\mathcal{X} \approx \mathcal{M} = \llbracket \boldsymbol{\lambda}; \mathbf{A}^{(1)}, \dots, \mathbf{A}^{(N)} \rrbracket = \sum_{r=1}^R \lambda_r \mathbf{a}_r^{(1)} \circ \dots \circ \mathbf{a}_r^{(N)}, \quad (1)$$

where $\boldsymbol{\lambda} = [\lambda_1, \dots, \lambda_R]$ is a scaling vector, $\mathbf{a}_r^{(n)}$ represents the r -th column of the factor matrix $\mathbf{A}^{(n)}$ of size $I_n \times R$, and \circ is the vector outer product. We refer to the operator $\llbracket \cdot \rrbracket$ as a Kruskal operator, and the tensor \mathcal{M} , with its specific multilinear model form, as a Kruskal tensor in (1). See [9] for more details regarding these definitions.

SparTen addresses the special case when the elements of \mathcal{X} are nonnegative counts. Assuming the entries in \mathcal{X} follow a Poisson distribution with multilinear parameters, the low-rank CP decomposition in (1) can be computed using the CP-APR methods, PDNR and PQNR, introduced by Hansen *et al.* [6].

3. Methods

In this section, we describe the hardware platforms, data, and SparTen algorithm parameters used in our experiments.

3.1 Hardware Platforms

We used diverse computer architectures running Red Hat Enterprise Linux (RHEL) to perform our experiments, with hardware and compiler specifications detailed in Table 1. Intel 1–4 are production clusters with hundreds to thousands of nodes, whereas ARM and IBM clusters are advanced architecture research testbeds with tens of nodes each. The ARM and IBM testbeds have larger memory and support many more threads per node than do any cluster in Intel 1-4. We employed the maximum number of OpenMP threads available per node from each platform to maximize throughput and configured the maximum wall-clock limit as 12:00 hours for all experiments. All parallelism was solely across threads on a single node. We built and compiled SparTen to leverage OpenMP via Kokkos with the latest software build tools available on each cluster. The GNU compiler, `gcc`, was used, with `-O3` optimization and Kokkos architecture-specific flags enabled.

Table 1: Hardware characteristics and software environment of the clusters in this paper. *Threads* and *RAM (GB)* are per node.

Platform	Processor	Nodes	CPUs	Threads	RAM (GB)	GCC
ARM	ThunderX2	44	28	256	255	7.2.0
IBM	Newell Power9	10	20	80	319	7.2.0
Intel 1	Sandy Bridge	1,848	29,568	16	64	8.2.1
Intel 2	Broadwell	740	26,640	36	128	8.2.1
Intel 3	Sandy Bridge	201	3,344	16	64	8.2.1
Intel 4	Sandy Bridge	1,232	19,712	16	64	8.2.1

3.2 Data

We conducted experiments using sparse tensors of count data from the FROSTT collection [11]. Specifically, we chose the following three datasets (summary statistics provided in Table 2) to account for size, dimensionality, and density (i.e., the ratio of nonzero entries to the total number of elements in the tensor):

1. Chicago Crime Community is a 4th-order tensor of crime reports in the city of Chicago spanning nearly 17 years. The four modes represent $day \times hour \times community \times crime-type$ and the values are counts.
2. LBNL-Network is a 5th-order tensor of anonymized internal network traffic at Lawrence Berkeley National Laboratory. The five modes represent $sender-IP \times sender-port \times destination-IP \times destination-port \times time$ and the values are total packet length per timestep.

- NELL-2 is 3rd-order benchmark tensor that gives a snapshot of the NELL: Never-Ending Language Learning relational database. The three modes represent *entity* \times *relation* \times *entity* relationships.

Throughout the discussion below, we refer to the data using the short names listed in the table.

Table 2: Sparse tensor datasets from the FROSTT collection.

FROSTT Name (short name)	Nonzeros	Dimensions	Density
Chicago Crime Community (<i>chicago</i>)	5.3M	(6186, 24, 77, 32)	1.5×10^{-02}
LBNL-Network (<i>lbnl</i>)	1.7M	(1605, 4198, 1631, 4209, 868131)	4.2×10^{-14}
NELL-2 (<i>nell</i>)	77M	(12092, 9184, 28818)	2.4×10^{-05}

3.3 Software Parameter Definitions & Experimental Ranges

PQNR and PDNR are composed of standard techniques in the numerical optimization literature. Specifically, for each tensor mode, the Newton optimization computes the gradient and Hessian matrix. Then, the inverse Hessian is approximated to compute a search direction and an Armijo backtracking line search is used to compute the Newton step. How the inverse Hessian is approximated differentiates PDNR and PQNR. PDNR shifts the eigenvalues by a damping factor μ to guarantee the Hessian matrix is semi-positive definite, and solves the resulting linear system exactly. PQNR approximates the inverse Hessian directly with a limited-memory BFGS (L-BFGS) approach, computed with a small number of update pairs. Since the algorithm parameters analyzed here are those presented in several equations and algorithms in [6], we defer to that paper for specific details.

To support discussion later in Section 4, we group the algorithm parameters into the following five categories. We note that the stability parameters used to safeguard against numerical errors—e.g., offset tolerances to avoid divide-by-zero floating point errors—do not appear in the corresponding Matlab Tensor Toolbox method `cp_apr`.

A. CP-APR

- `max_outer_iterations`: Maximum number of outer iterations to perform (Algorithm 1, Steps 2-9 in [6]).
- `max_inner_iterations`: Maximum number of inner iterations to perform (K_{max} in Algorithms 3 and 4 in [6]).

B. Line search

- `max_backtrack_steps`: Maximum number of backtracking steps in line search (maximum allowable value of t used in Equation (17) in [6]).
- `min_variable_nonzero_tolerance`: Tolerance for nonzero line search step length (smallest allowable value of β in Equation (17) in [6]).
- `step_reduction_factor`: Factor to reduce line search step size between iterations (β^{t+1}/β^t in Equation (17) in [6]).

- `suff_decrease_tolerance`: Tolerance to ensure the next iterate decreases the objective function (σ in Equation (17) in [6]).

C. Damped Newton (PDNR)

- `mu_initial`: Initial value of damping parameter (μ_0 in Algorithm 3 in [6]).
- `damping_increase_factor`: Scalar value to increase damping parameter in next iterate (Equation (16) in [6]).
- `damping_decrease_factor`: Scalar value to decrease damping parameter in next iterate (Equation (16) in [6]).
- `damping_increase_tolerance`: Tolerance to increase the damping parameter (Equation (16) in [6]). If the search direction increases the objective function and the ratio of actual reduction and predicted reduction in objective function (ρ in Equation (15) in [6]) is less than `damping_increase_tolerance`, the damping parameter μ_k will be increased for the next iteration.
- `damping_decrease_tolerance`: Tolerance to decrease the damping parameter (Equation (16) in [6]). Conversely, if the search direction decreases the objective function and the ratio of actual reduction to predicted reduction (ρ in Equation (15) in [6]) is greater than `damping_decrease_tolerance`, the damping parameter μ_k will be decreased for the next iteration.

D. Quasi-Newton (PQNR)

- `size_LBFGS`: Number of recent limited-BFGS (L-BFGS)-update pairs to use in estimating the current Hessian (M in Equation (18) in [6]).

E. Numerical stability

- `eps_div_zero_grad`: Safeguard against divide-by-zero in gradient and Hessian calculations.
- `log_zero_safeguard`: Tolerance to avoid computing $\log(0)$ in objective function calculations.

The default value in SparTen of each parameter described above and the experimental ranges tested in these experiments are given in Table 3.

3.4 Experiments

An individual experiment is a job j on platform m solving a PDNR/PQNR row subproblem for dataset d with SparTen solver s , parameter p , parameter value v , and random initialization r ; all remaining software parameters are fixed at the default values listed in Table 3. Certain experiments denoted with a dagger[†] were run only on Intel hardware due to limited resources associated with the other architectures; this accounts for the larger number of experiments reported for these platforms. We conducted tests on these values to provide better resolution of the impact of the parameter where nearby values—i.e., on the bounds

Table 3: SparTen software parameter descriptions and values used in our experiments.

Parameter	Default	Values Used in Experiments
<code>max_outer_iterations</code> ¹	10 ⁵	1, 2, 4, 8, 16, 32, 64, 128, 256, 512
<code>max_inner_iterations</code> ¹	20	20, 40, 80, 160
<code>max_backtrack_steps</code> ²	10	1 [†] , 2, 4, 8, 10, 12 [†] , 16
<code>min_variable_nonzero_tolerance</code> ²	10 ⁻⁷	10 ^{-1†} , 10 ⁻³ , 10 ⁻⁷ , 10 ^{-15†}
<code>step_reduction_factor</code> ²	0.5	0.1, 0.3 [†] , 0.5, 0.7 [†] , 0.9
<code>suff_decrease_tolerance</code> ²	10 ⁻⁴	10 ⁻² , 10 ⁻⁴ , 10 ^{-8†} , 10 ^{-12†}
<code>mu_initial</code> ³	10 ⁻⁵	10 ⁻² , 10 ⁻⁵ , 10 ⁻⁸
<code>damping_increase_factor</code> ³	3.5	1.5, 2.5 [†] , 3.5, 4.5 [†] , 5.5
<code>damping_decrease_factor</code> ³	2/7	0.1, 2/7, 0.3 [†] , 0.5, 0.7 [†] , 0.9
<code>damping_increase_tolerance</code> ³	0.25	0.1, 0.25, 0.495
<code>damping_decrease_tolerance</code> ³	0.75	0.505, 0.75, 0.9
<code>size_LBFGS</code> ³	3	1, 2, 3, 4, 5, 10, 15, 20
<code>eps_div_zero_grad</code> ⁴	10 ⁻¹⁰	10 ⁻⁵ , 10 ^{-8†} , 10 ⁻¹⁰ , 10 ^{-12†} , 10 ⁻¹⁵
<code>log_zero_safeguard</code> ⁴	10 ⁻¹⁶	10 ^{-4†} , 10 ⁻⁸ , 10 ^{-12†} , 10 ⁻¹⁶ , 10 ^{-24†} , 10 ⁻³²
<code>eps_active_set</code> ⁴	PDNR: 10 ⁻³ PQNR: 10 ⁻⁸	10 ⁻¹ , 10 ⁻³ , 10 ^{-5†} , 10 ^{-8†} 10 ⁻¹ , 10 ⁻³ , 10 ^{-5†} , 10 ^{-8†}

¹⁻⁴Intel platform used for experiments; [†]values evaluated on Intel platform only

of the test range—contained uncertainty in the results. Furthermore, we split up the experiments across the Intel platforms by parameter, running the full set of experiments across all parameter values and all random initializations on a single platform. The superscripts denoted for each parameter in the table denote the Intel platform number specified in Table 1. Since we report only the number of function evaluations and outer iterations in our results, we expect that running our experiments in this way has produced valid results.

In all experiments, we fit a 5-component CP decomposition using a tolerance of 10⁻⁴ (i.e., the value of τ in Equation (20) in [6], the violation of the Karush-Kuhn-Tucker (KKT) conditions, used as the stopping criterion for the methods we explore here). Computation of a CP decomposition using PDNR or PQNR in SparTen requires an initial guess of the model parameters—i.e., initial values for \mathcal{M} in (1)—drawn from a uniform distribution in the range [0, 1]. As such, all experiments were replicated using 30 random initializations. We report results on the amount of computation required for convergence (i.e., the number of evaluations of the negative log likelihood objective function, $f(\mathcal{M})$, defined in Equation (4) of [6]) and the quality of the solution (i.e., the value of the negative log likelihood objective function). As each of our experiments consists of 30 replicates (i.e., 30 random initializations) across three CPU architectures, we report sample means and 95% confidence intervals (as defined in [10]) when presenting statistical trends in the results.

4. Results

Table 4: Experiments run on the different datasets and hardware platforms.

CPU	Solver	Data	Planned	Collected	Canceled	Converged	Max Iterations	Missing
ARM	PDNR	<i>chicago</i>	1110	1110	4.8%	82.2%	13.0%	0.0%
		<i>lbnl</i>	1110	1110	10.5%	76.5%	13.0%	0.0%
		<i>nell</i>	1110	390	5.4%	39.2%	55.4%	64.9%
	PQNR	<i>chicago</i>	990	281	0.0%	55.5%	44.5%	71.6%
		<i>lbnl</i>	990	237	0.0%	0.0%	100.0%	76.1%
		<i>nell</i>	990	390	23.3%	0.3%	76.4%	60.6%
IBM	PDNR	<i>chicago</i>	1110	855	5.4%	77.8%	16.8%	23.0%
		<i>lbnl</i>	1110	692	11.3%	73.3%	15.4%	37.7%
		<i>nell</i>	1110	424	51.2%	12.0%	36.8%	61.8%
	PQNR	<i>chicago</i>	990	676	10.2%	76.3%	13.5%	31.7%
		<i>lbnl</i>	990	293	61.8%	0.0%	38.2%	70.4%
		<i>nell</i>	990	481	31.0%	6.6%	62.4%	51.4%
Intel	PDNR	<i>chicago</i>	1680	1673	5.0%	86.4%	8.6%	0.4%
		<i>lbnl</i>	1680	1663	11.0%	80.6%	8.4%	1.0%
		<i>nell</i>	1680	1643	44.7%	42.2%	13.1%	2.2%
	PQNR	<i>chicago</i>	1440	1434	12.1%	78.6%	9.3%	0.4%
		<i>lbnl</i>	1440	1363	78.0%	0.0%	22.0%	5.3%
		<i>nell</i>	1440	1424	68.8%	10.1%	21.1%	1.1%

In this section we analyze the results of the parameter sensitivity experiments and describe the statistical relationships between the convergence properties of the PDNR and PQNR methods and their input parameters.

In total, 21,960 unique experiments were planned, accounting for running PDNR and PQNR with random initializations across all parameter value ranges on the various hardware architectures described in Sections 3.1 and 3.3. An experiment *converged* if the final KKT violation is less than the value of $\tau = 10^{-4}$; an experiment reached *maximum iterations* if the number of outer iterations exceeded the maximum limit (i.e., `max_outer_iterations`) and did not converge; an experiment was *canceled* if it exceeded the wall-clock limit (i.e., SparTen neither converged to a solution nor reached maximum number of outer iterations within 12 hours); and an experiment was *missing* if it did not run due to a failure of the system to launch the experiment or other system issue. Of the planned experiments, we collected data from 16,139 experiments.

Table 4 presents the number of experiments planned as defined above and the number of planned experiments where data was collected (i.e., planned minus missing). For those collected, the table shows the percentage of experiments that were canceled, converged, or exceeded the maximum iterations. We note that the most complete set of experiment results were obtained on the Intel platforms. Although there are many missing experiment results for the IBM and ARM platforms, we attempt to identify patterns in the data we collected if there is strong evidence to support our claims. We note that a few parameters (`eps_active_set`, `min_variable_nonzero_tolerance`, `suff_decrease_tolerance`, `damp-`

ing_increase_tolerance, damping_decrease_tolerance) showed no statistically significant differences across the range of input values used in the experiments. We conjecture that we did not find values where the parameters display sensitivities in the chosen tensor problems, thus it remains unclear if this behavior holds in general.

4.1 General Convergence Results on Real-World Data

To illustrate general convergence behavior, we present the results of the experiments in a heatmap for a given dataset, method, and hardware platform. Figure 1 presents an example heatmap, where each square represents the total number of objective function evaluations of an experiment, with random initializations across the rows and parameter values used (with all other parameter values set to their default values) across the columns. The complete set of heatmaps for all experiments can be found in Appendix A.1. These results illustrate that there are certain ranges of parameter values that lead to good or bad convergence behaviors in general.

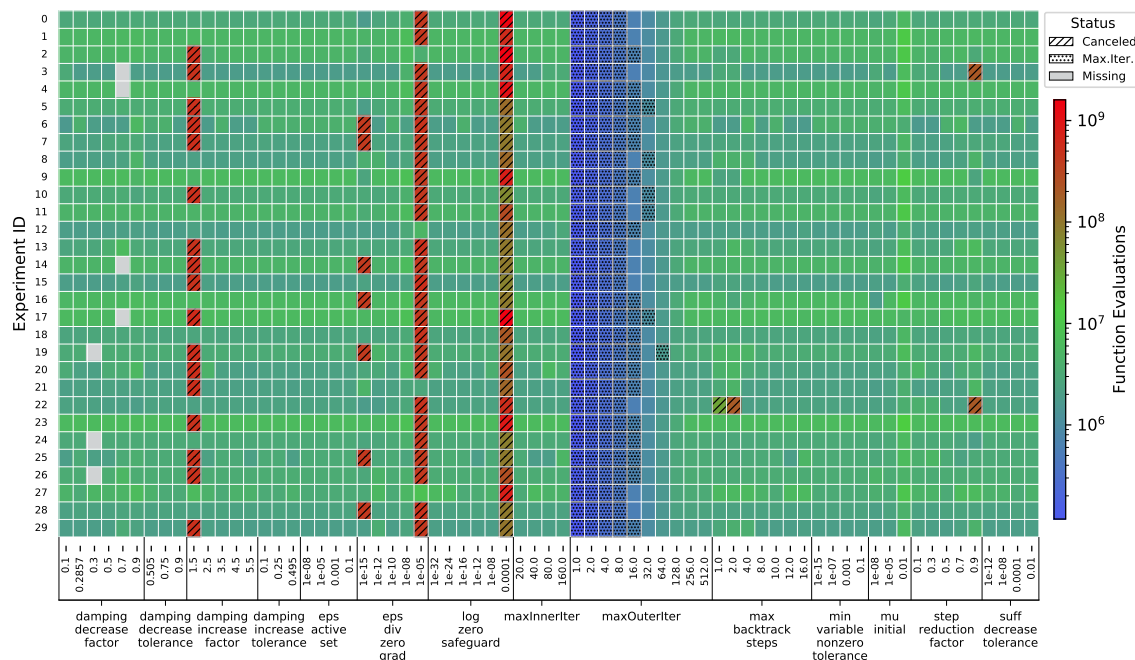


Figure 1: Example heatmap illustrating results.

The colours in the heatmaps denote the outcomes of the experiments as follows. Green shades are consistent with *converged* experiments. Vertical bands not shaded green identify values that may impact algorithm performance, due either to iteration constraints (blue hues) or excessive computations corresponding to slow convergence or stagnation (red hues). Hatches denote non-convergent exit status. Grey represents *missing* data, i.e., experiments that were planned but never conducted due to resource limitations—e.g., dequeued by the cluster administrator—or a system failure. Solid columns of a single shade indicating the same convergence behavior across all 30 random initializations. Nearly solid column lines

of the same shade indicate similar behavior, but also that there is some sensitivity of those parameter values to the initial starting point of the iterative methods.

Observation 1: Convergence properties are demonstrated empirically. As discussed in Section 1, applying PDNR and PQNR to real-world data has been explored previously in the literature only for a single problem. From Table 4, we observed that PQNR is canceled more than PDNR in the allotted time across datasets and CPU platforms. This confirms our intuition, since it is a classical result in iterative methods that damped Newton methods converge quadratically, in comparison to quasi-Newton methods, which converge superlinearly. Specifically, PQNR calls the objective function 2.7 times more than PDNR on average on the *chicago* data and fails to converge in the allotted time for any experiment on *lbnl* data across all hardware platforms. By contrast, PDNR converges in 86% of *lbnl* experiments across platforms when only 32 outer iterations are allowed.

Observation 2: There is consistent convergence behavior across many ranges of parameter values. Looking across the range of values for each parameter, there are many cases where there is a distinct change in behavior—e.g., from converged to canceled when `log_zero_safeguard` is greater than 10^{-8} in PDNR experiments on *chicago* as shown in Figure 5. This distinct, repeatable behavior can be used to guide the choices for both a general set of parameter defaults and tuning of parameters for specific data.

Observation 3: PDNR and PQNR are not necessarily sensitive to the same parameters. In some cases PQNR converges where PDNR is canceled using the same random initial starting point. Several interesting patterns from the *nell* results should also be noted. First, the solution space is highly sensitive to random initialization (seen as hatched red bands in Figure 7). Thus statements quantifying average behavior are more uncertain. Second, where PQNR does converge on *nell*, it is for extreme values where convergence is unlikely in other cases—for example, using the following parameter values:

- `eps_div_zero_grad` $\leq 10^{-12}$,
- `log_zero_safeguard` $\geq 10^{-8}$,
- `max_backtrack_steps` ≤ 4 .

In the next section, we present analysis of the results that expands on these observations.

4.2 Sensitivity of Convergence and Solution Behavior

We are interested in comparing the convergence results across parameter values and solvers. In the following sections, we will refer to Tables 5, 6, and 7, which compare the computational costs between PDNR and PQNR by reporting the mean number of objective function evaluations of *converged* jobs from the three data sets for each parameter value on all computer hardware platforms with 95% confidence intervals presented as percentages above and below the mean. We proceed by analyzing the results by the categories of parameters described in Section 3.3: general CP-APR parameters, line search parameters, damped Newton step parameters, Quasi-Newton step parameters, and numerical stability parameters.

4.2.1 CP-APR

As noted above, damped Newton methods converge faster than Quasi-Newton methods (quadratic convergence versus super-linear, respectively). Thus, we are interested in determining the impact on convergence of constraining the maximum number of allowable iterations in the outer and inner solvers. Note that in experiments that do not measure the effect of `max_outer_iterations` and `max_inner_iterations` explicitly, these values were fixed at 100,000 and 20, respectively.

In all cases, there is a minimum value where PDNR converges to a solution. However, PQNR times out for all `max_outer_iterations` test values on *lbnl* and *nell*. Where comparisons can be made (*chicago*), PQNR calls the objective function 2.7 times more than PDNR on average, although this relative cost between solvers decreases as `max_outer_iterations` grows.

The effect of increasing the maximum number of inner iterations, `max_inner_iterations`, is similar. The non-monotonic increase in function evaluations for the maximum number of inner iterations can be explained by the trade-off between outer and inner iterations depending on a particular data set. The exception to this trend is the result that PDNR calls the objective function 2.33 times more than PQNR on *nell* (see Table 7), although this is most likely due to so few converged PQNR experiments and may not be statistically significant.

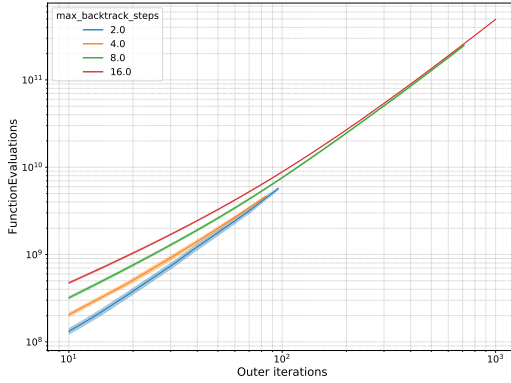
In principle, there is a value of parameter `eps_active_set` that will have an effect on convergence. In practice, however, we did not find that value for any dataset. We note that this result differs from [6], which found setting the parameter to 10^{-3} leads to faster PDNR convergence, compared to a value of 10^{-8} . Therefore, since algorithm sensitivity to this parameter is data-dependent, it is unreasonable to generalize behavior.

4.2.2 LINE SEARCH

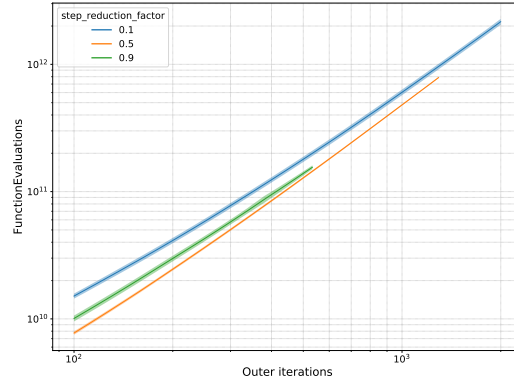
Allowing many backtracking steps during the line search, set by `max_backtrack_steps` may cause PDNR to waste effort; however, PQNR appears to perform better, in general, with more steps. PDNR is sensitive to the number of backtracking steps on *chicago*: average work performed is less when the maximum number of allowed steps is large and more work is performed when the number of steps is small. On *lbnl*—the sparsest tensor problem considered—PDNR performs better with fewer backtracking steps (see Figure 2a).

The line search parameter `step_reduction_factor` is used to reduce the line search step size between iterations (β^{t+1}/β^t in Equation (17) in [6]). On a large, sparse tensor problem, increasing this parameter may accelerate convergence. On the other hand, a small value makes convergence less certain. Figure 2b illustrates this behavior on the *lbnl* data: the average total cost decreased by 77% as `step_reduction_factor` increased from 0.1 to 0.5 (SparTen default) and decreased another 28% from 0.5 to 0.9. On *nell* data, PQNR *only* converged for large values (0.7, 0.9).

Threshold parameter `min_variable_nonzero_tolerance` guarantees that the final Newton step length is nonzero. In theory, if this value is too large, the next iterate may overstep important information, forcing additional iterations to correct the misstep. On the other hand, if the value is too small, the algorithm may converge too slowly. We observed no statistically significant differences in PDNR algorithm performance when varying this pa-



(a) The x -axis is truncated to emphasize the lower average cost when fewer `max_backtrack_steps` are allowed; the figure does not fully capture the high average cost when 16 maximum backtrack steps are allowed (PDNR, *lbnl*).



(b) The x -axis is truncated to demonstrate how high `step_reduction_factor` may accelerate convergence on large, sparse tensor data (PDNR, *lbnl*).

parameter on *chicago*. The same appears true for PQNR, although we caution that empirical data is limited to results on *chicago* only. Addressing the result that no experiments converged for `min_variable_nonzero_tolerance` 10^{-1} or 10^{-15} on *nell*, it is unlikely that size and sparsity play a role in parameter convergence; PDNR algorithm performance shows no significant difference on *lbnl*, the largest and sparsest tensor problem.

The parameter `suff_decrease_tolerance` is used to assess if sufficient decrease in the objective function has been achieved in the line search—i.e., it is used to determine when to stop the line search iterations. A characterization virtually identical to that made for parameter `min_variable_nonzero_tolerance` can also be stated here. In short, there is no significant performance difference when varying this parameter on PDNR or PQNR, although PQNR results are limited to *chicago* only.

4.2.3 DAMPED NEWTON (PDNR)

In this section, we discuss results of varying parameters that are used only by the PDNR solver. The damped Newton parameters control updates to the damping factor for the next iterate (μ_k in Equation (16) in [6]). The damping parameter μ_k shifts the eigenvalues of the Hessian matrix, forcing it to be positive semidefinite and guaranteeing that a solution exists. For every outer iteration, the damping factor is initialized to `mu_initial` and updated using the following parameters:

1. `damping_decrease_factor`
2. `damping_decrease_tolerance`
3. `damping_increase_factor`
4. `damping_increase_tolerance`

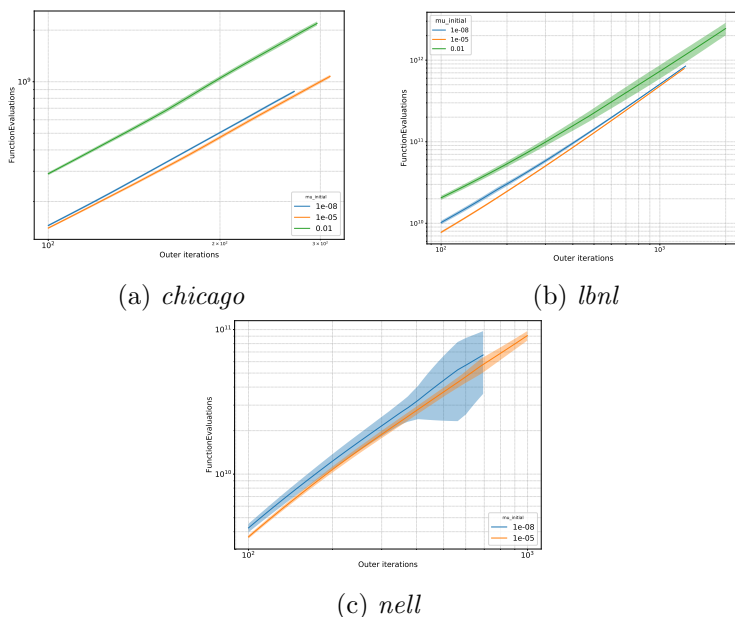


Figure 3: PDNR, `mu_initial`. Mean function evaluations and 95% CI. PDNR damps out Hessian information and is more prone to time-outs when `mu_initial` is large (PDNR, *lbnl*).

Hansen *et al.* predict in [6] that when the damping parameter μ is set too large, a loss of Hessian information follows, which impacts convergence:

“We expect larger values of μ_k to improve robustness by effectively shortening the step length and hopefully avoiding the mistake of setting too many variables to zero. However, a serious drawback to increasing μ_k is that it damps out Hessian information, which can hinder the convergence rate.”

For example, when `mu_initial` is large, the computational cost grows dramatically and time-outs become more likely, since the initial step length will at first be very small in every outer iteration and useful Hessian information is discarded in early stages of the inner loop solves. See Figure 3. Convergence is most likely for a large, but not too-large, value, i.e., `mu_initial` = 10^{-5} . Cost grows 177.2% on *lbnl* and nearly doubles (+92.2%) on *chicago* as `mu_initial` grows from 10^{-5} to 10^{-2} . It is important to note in the former case that this cost is skewed by one experiment that converged after nearly 42,000 outer iterations, in comparison to 1,300 for the other parameter values on average, illustrated in Figure 3, where the x -axis is truncated to highlight the differences in total cost. Smaller values (i.e., 10^{-8}) seem to perform better for *chicago*, the smallest, densest problem and larger values (i.e., 10^{-5}) tend to perform better for large, sparse problems.

PDNR parameters `damping_increase_factor` and `damping_decrease_factor`, which control updates to the Hessian matrix damping parameter μ , are two examples of algorithm parameters where convergence behavior is similar for values set within sensitivity constraints. SparTen rarely converges when the former is set too low (1.5); the likely effect is that the updated damping factor is insufficient to guarantee a well-conditioned Hessian

and too many unimportant directions are considered when computing the search direction. Above the 1.5 bound, the cost in objective function calls does not change significantly.

In our experiments, we found that varying either `damping_decrease_tolerance` or `damping_increase_tolerance` has no noticeable effect on either the number of calls to the objective function nor the number of outer iterations performed.

4.2.4 QUASI-NEWTON (PQNR)

In this section, we discuss varying parameter `size_LBFGS`, which is the only software parameter used by the PQNR solver. PQNR uses a limited memory BFGS (L-BFGS) approach to approximate the inverse Hessian matrix in the Quasi-Newton step, with M update pairs stored. The value of M is set by the parameter `size_LBFGS`. See [6] for algorithm details. More update pairs M should provide a higher resolution to approximate the inverse Hessian. Intuitively, too few update pairs seems insufficient to compute an acceptable approximation. The only observable difference occurs when the update size is 1, using only the current iterate in the BFGS update.

4.2.5 NUMERICAL STABILITY

The numerical stability parameters `eps_div_zero_grad` and `log_zero_safeguard` described in this Section are offset tolerances to avoid divide-by-zero floating point errors tailored to SparTen’s C++ implementation. They do not appear in the corresponding Matlab Tensor Toolbox method `cp_apr`. Their impact on convergence was consistent across combinations of solver, data, and CPU hardware.

The parameter `eps_div_zero_grad` is an offset to avoid divide-by-zero floating point errors when computing the gradient and Hessian (Equation (10) in [6]). When `eps_div_zero_grad` is large, gradient directions that do not lead to objective function improvements may be scaled the same as gradient directions that do lead to such improvements. Furthermore, the corresponding eigenvalues of the Hessian matrix are amplified and Hessian information may be lost when determining the next iterate. For example, PDNR loses Hessian information as `eps_div_zero_grad` increases on *chicago* data; PDNR rarely converges and PQNR never converges when this parameter is relatively large—i.e. 10^{-5} . Moreover, both algorithms are sensitive to the parameter’s lower bound, as small values may be insufficient to avoid an ill-conditioned Hessian matrix. In either case, additional iterations follow to correct errors incurred by `eps_div_zero_grad` values, large and small.

Parameter sensitivities affect not only convergence behavior, but may also produce qualitatively different results. Figure 4 illustrates the effect where large `eps_div_zero_grad`—and consequently, small step length—minimizes calls to the objective function *and* results in minimal objective function value. Most striking is that larger `eps_div_zero_grad` decreases the objective function more than an order of magnitude. This result was collected from 79 of 90 planned PDNR experiments on *lbnl*, and thus we consider this interesting effect worthy of further investigation.

PDNR typically does not converge for large `log_zero_safeguard` values on large tensor problems. This parameter sets a nonzero offset in logarithm calculations to avoid explicitly computing $\log(0)$. High precision in logarithm computations tends to ensure the objective function is minimized accurately. When the value is too large, the calculated logarithm

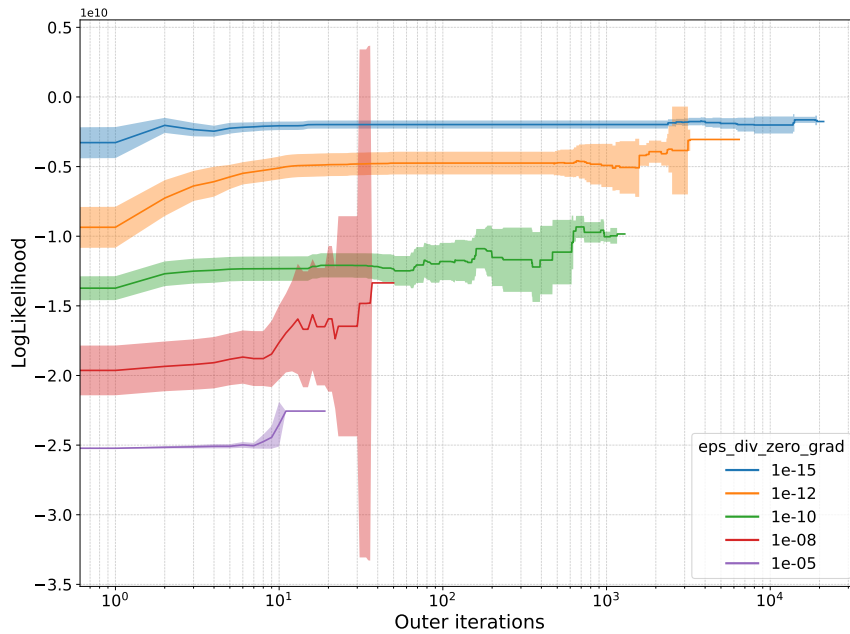


Figure 4: Mean objective function values with 95% confidence interval, varying `eps_div_zero_grad` (PDNR, *lbnl*).

may be too small, and more backtracking steps are required to sufficiently decrease the objective function in the line search routine, making time-outs more likely. On the other hand, the effect of the parameter on convergence is indistinguishable for values smaller than 10^{-8} across all experiments.

5. Conclusions

Using results from more than 16,000 numerical experiments on several hardware platforms, we presented experimental results that expand our understanding of average PDNR and PQNR convergence on real-world tensor problems. We have shown that when using PQNR to compute large tensor decompositions convergence is less-likely under reasonable resource constraints. We have shown that some software parameters are sensitive to bounds on values. Further, we showed that varying several parameters can dramatically impact algorithm performance, and in some cases, may produce qualitatively different results.

Future work may address the issue of stagnation in Newton optimization methods for CP decompositions. We showed examples where the solver converged to a solution slowly but within the allotted time of 12 hours. For those experiments that timed out, it is unknown whether SparTen would eventually converge to a solution or stagnate without making progress. We anticipate that stagnation could be determined if the objective function values converge to a statistical steady state without satisfying the convergence criterion. Future development of SparTen may include dynamic updates to algorithm parameters based on local convergence information. Lastly, future experiments could explore coupled sensitivities among algorithm parameters, as this work was limited to single parameter, univariate analyses. Understanding the nature of bivariate (or even more complex) relationships among parameters may better inform end-users when searching for optimal parameter choices to run the SparTen methods.

References

- [1] Brett W. Bader, Tamara G. Kolda, et al. Matlab tensor toolbox version 3.0-dev. Available online, August 2017.
- [2] J.D. Carroll and J. Chang. Analysis of individual differences in multidimensional scaling via an n-way generalization of “eckart-young” decomposition. *Psychometrika*, 35:283–319, 1970.
- [3] A. Cichocki, D. Mandic, L. De Lathauwer, G. Zhou, Q. Zhao, C. Caiafa, and H. A. PHAN. Tensor decompositions for signal processing applications: From two-way to multiway component analysis. *IEEE Signal Processing Magazine*, 32(2):145–163, 2015.
- [4] Leonardo Dagum and Ramesh Menon. Openmp: an industry standard api for shared-memory programming. *Computational Science & Engineering, IEEE*, 5(1):46–55, 1998.
- [5] H. Carter Edwards, Christian R. Trott, and Daniel Sunderland. Kokkos: Enabling manycore performance portability through polymorphic memory access patterns. *Journal of Parallel and Distributed Computing*, 74(12):3202–3216, 2014. Domain-Specific Languages and High-Level Frameworks for High-Performance Computing.
- [6] Samantha Hansen, Todd Plantenga, and Tamara G. Kolda. Newton-based optimization for Kullback-Leibler nonnegative tensor factorizations. *Optimization Methods and Software*, 30(5):1002–1029, April 2015.
- [7] Richard A. Harshman. Foundations of the PARAFAC procedure: models and conditions for an “explanatory” multi-modal factor analysis. *UCLA Working Papers in Phonetics*, 16(1):84–84, 1970.
- [8] Frank L. Hitchcock. The expression of a tensor or a polyadic as a sum of products. *Journal of Mathematics and Physics*, 6(1–4):164–189, 1927.
- [9] T. Kolda and B. Bader. Tensor decompositions and applications. *SIAM Review*, 51(3):455–500, 2009.
- [10] Lawrence M. Leemis and Stephen K. Park. *Discrete-Event Simulation: A First Course*. Prentice-Hall, Inc., USA, 2005.
- [11] Shaden Smith, Jee W. Choi, Jiajia Li, Richard Vuduc, Jongsoo Park, Xing Liu, and George Karypis. Frostt: The formidable repository of open sparse tensors and tools. Available online, 2017.

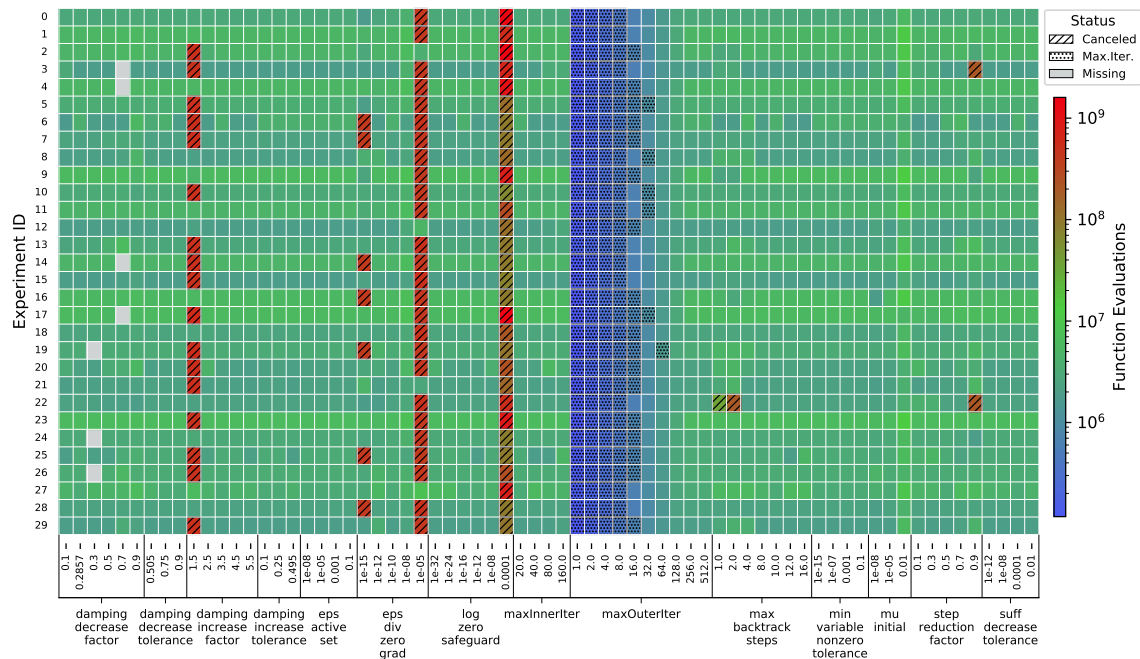
Appendix A. Detailed Experiment Results

This section provides additional results for the experiments described in this analysis.

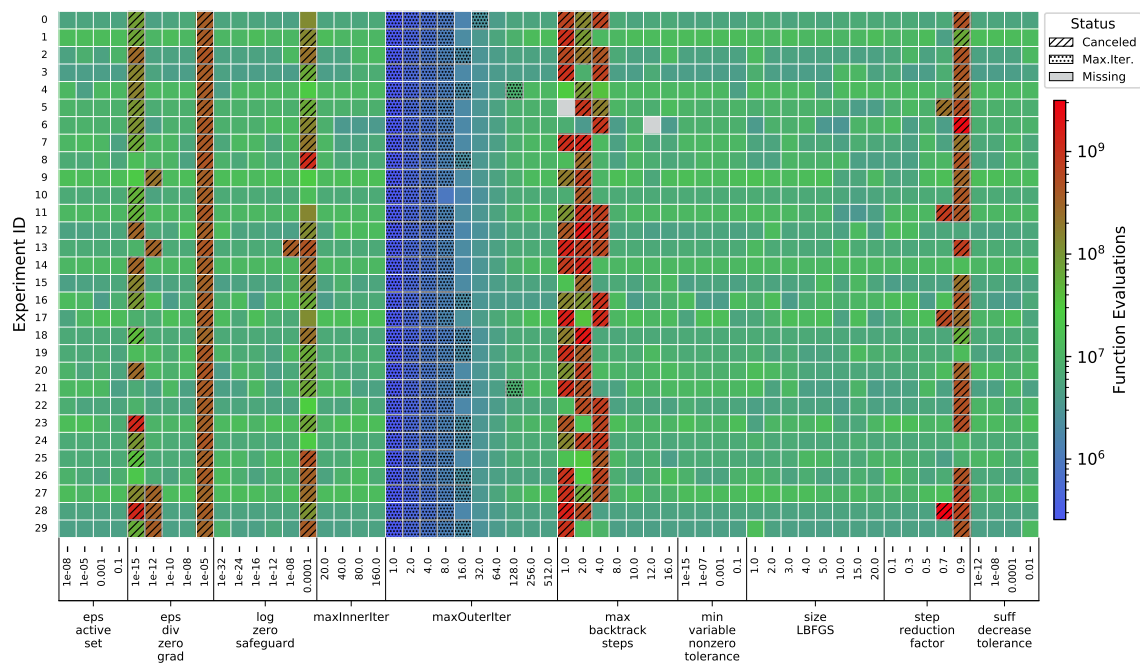
A.1 Heatmaps

Below are the outcomes of the planned experiments described in this report presented as heatmap images. They are organized by hardware platform, data set and solver used in each experiments, as described in Section 3.

Figure 5: Experiment outcomes for *chicago-crime-comm* data on Intel platform.

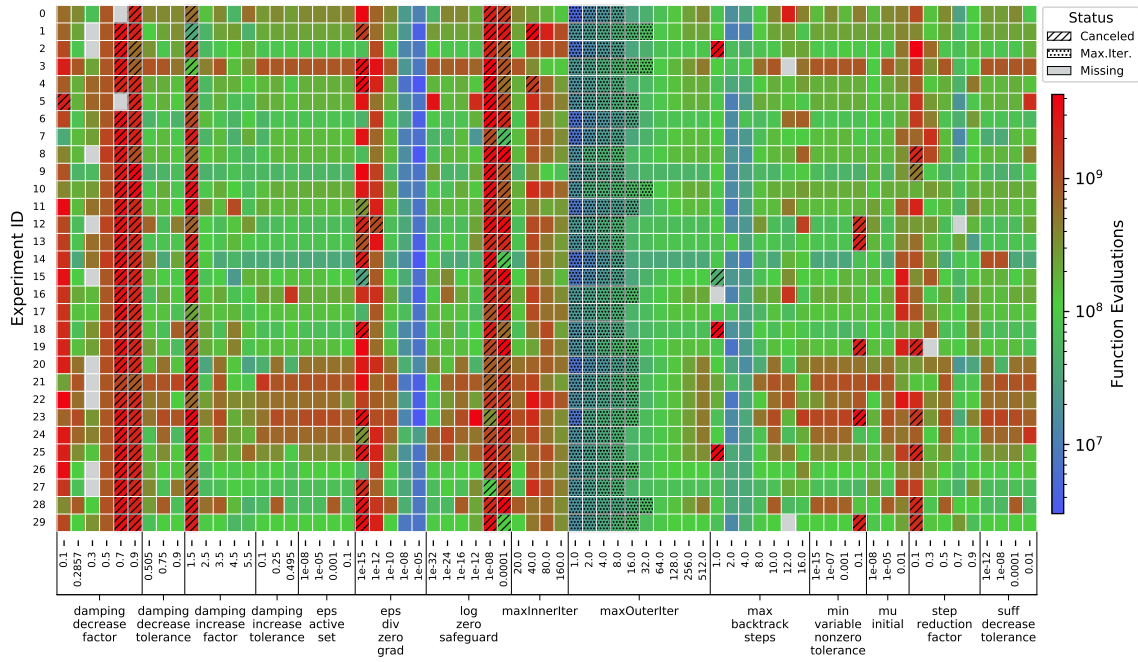


(a) PDNR

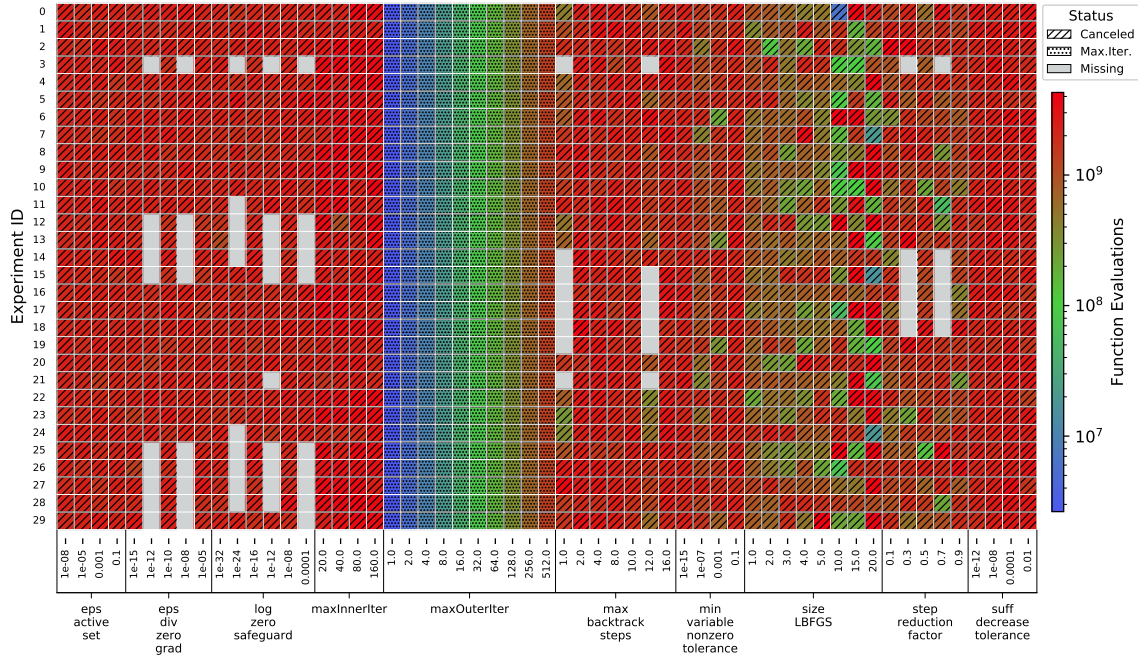


(b) PQNR

Figure 6: Experiment outcomes for *lbnl-network* data on Intel platform.

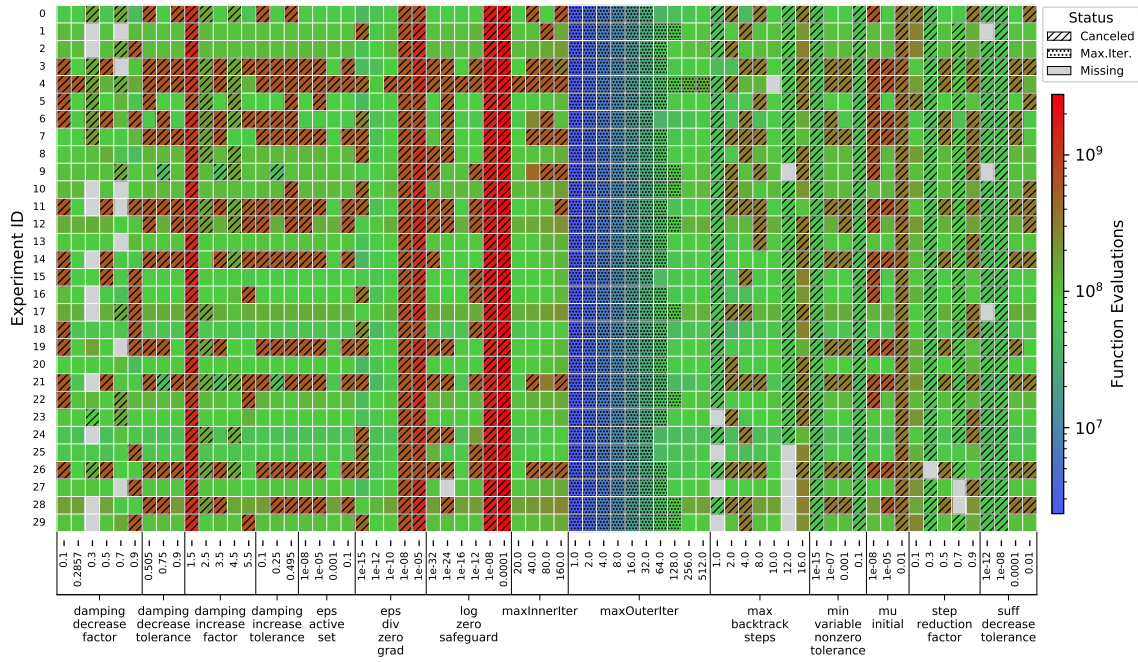


(a) PDNR

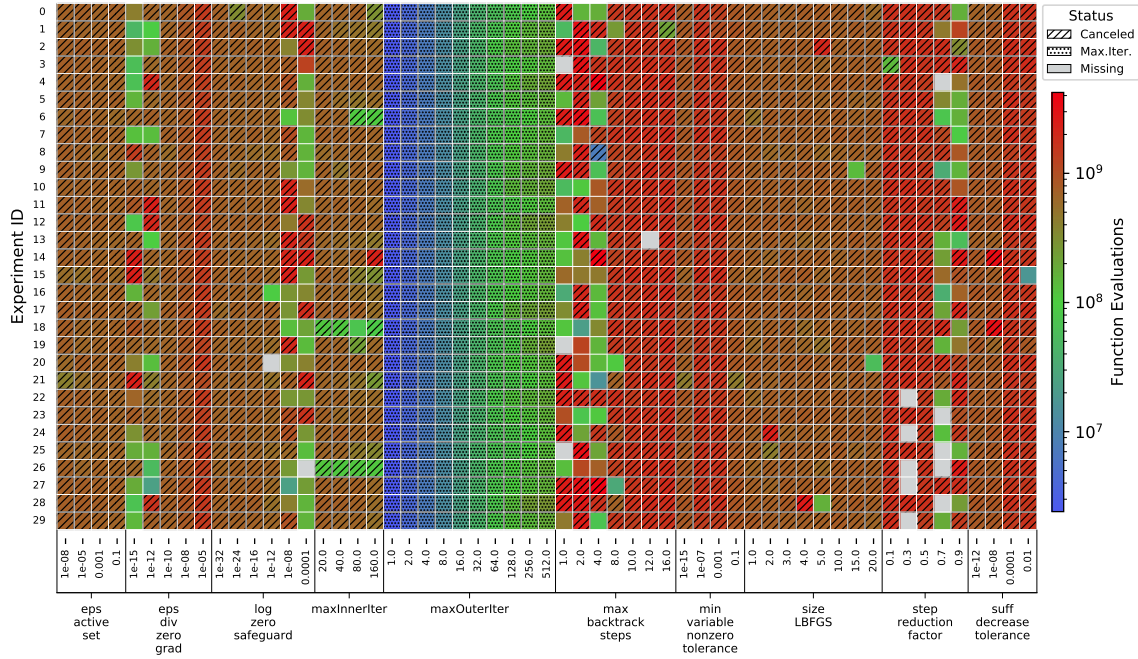


(b) PQNR

Figure 7: Experiment outcomes for *nell-2* data on Intel platform.

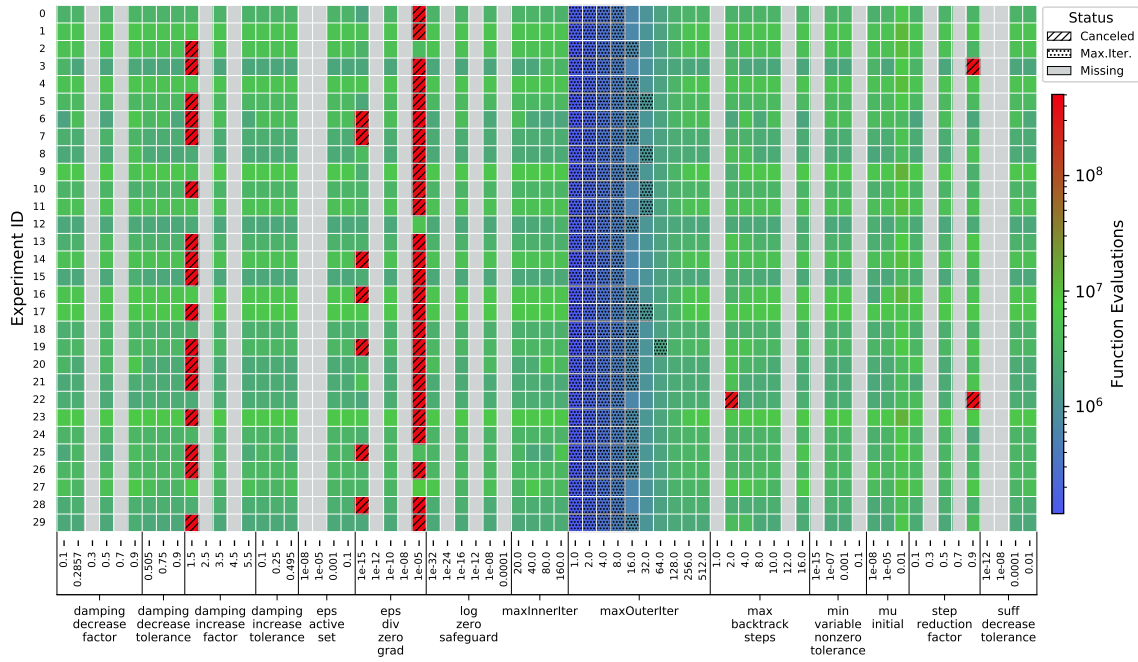


(a) PDNR

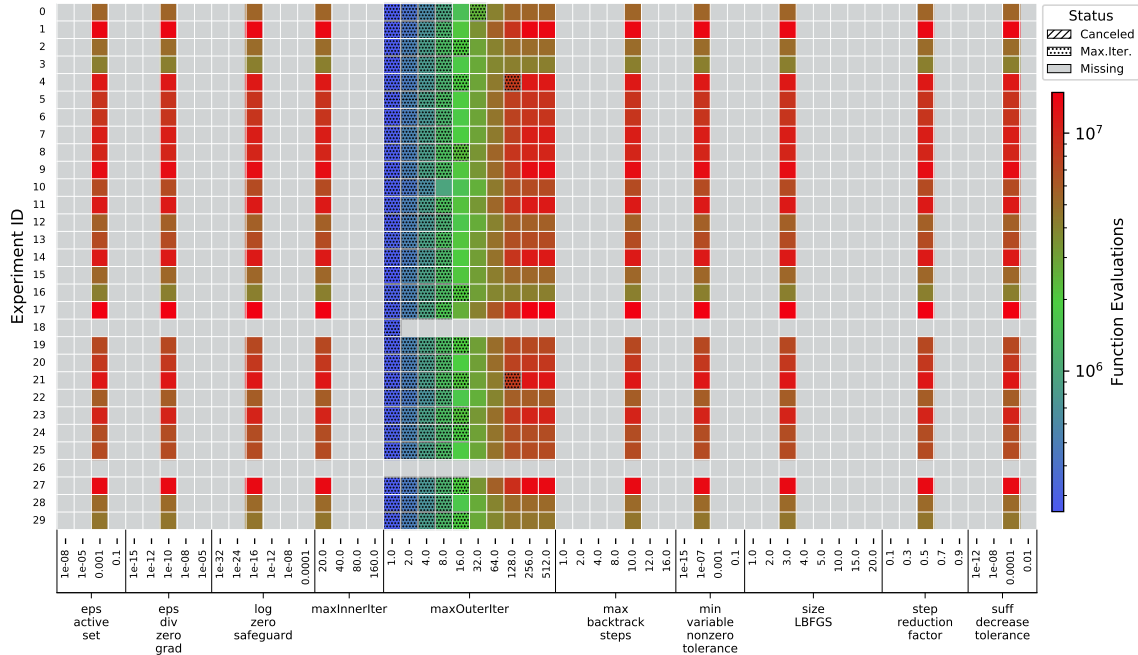


(b) PQNR, *nell-2*

Figure 8: Experiment outcomes for *chicago-crime-comm* data on ARM platform.

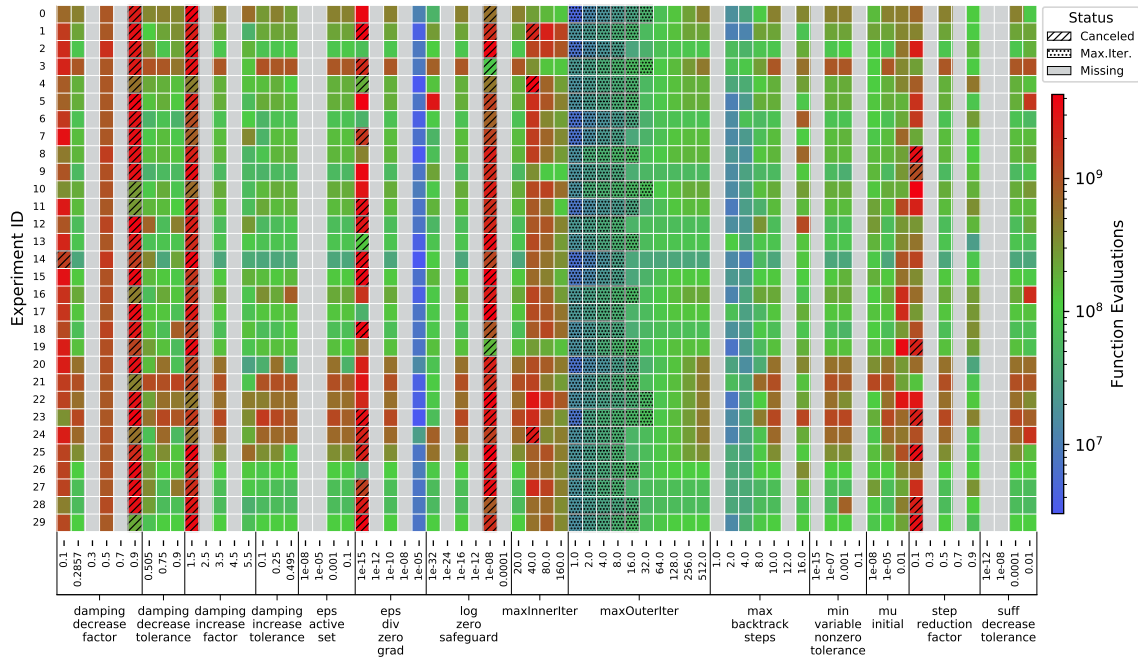


(a) PDNR, *chicago-crime-comm*

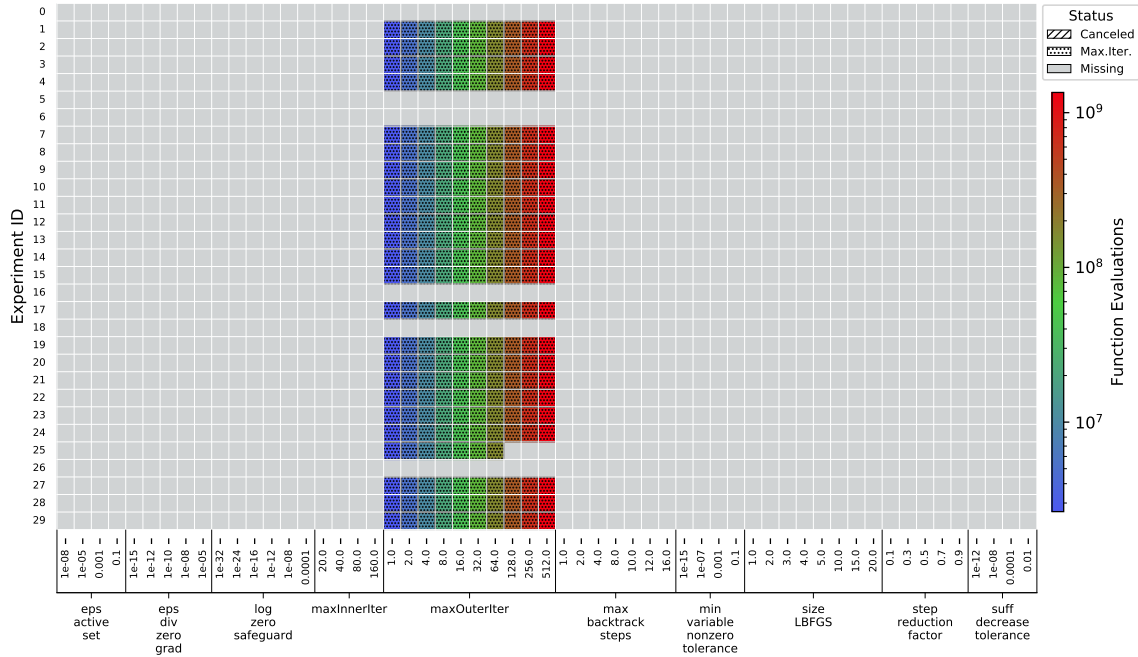


(b) PQNR, *chicago-crime-comm*

Figure 9: Experiment outcomes for *lbnl-network* data on ARM platform.

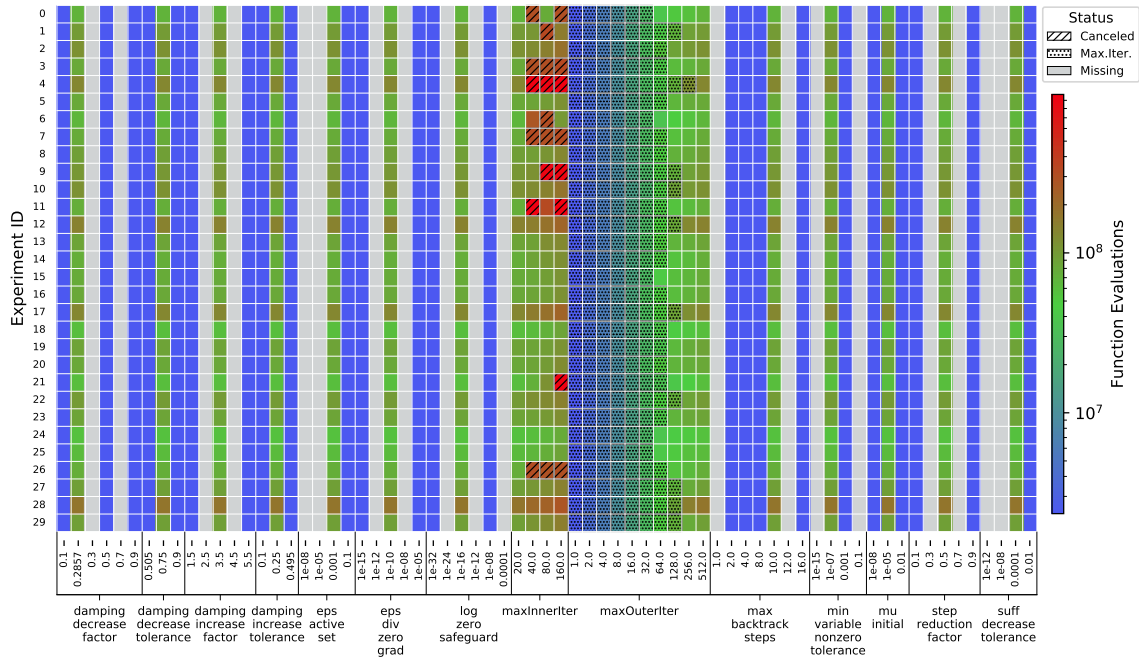


(a) PDNR, *lbnl-network*

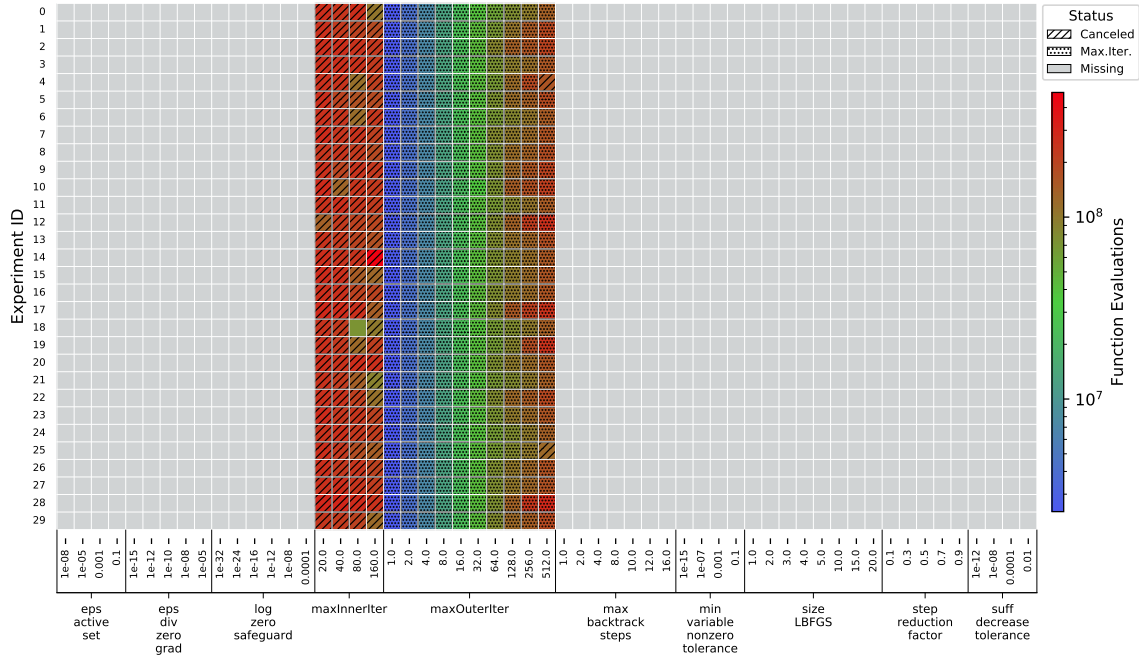


(b) PQNR, *lbnl-network*

Figure 10: Experiment outcomes for *nell-2* data on ARM platform.

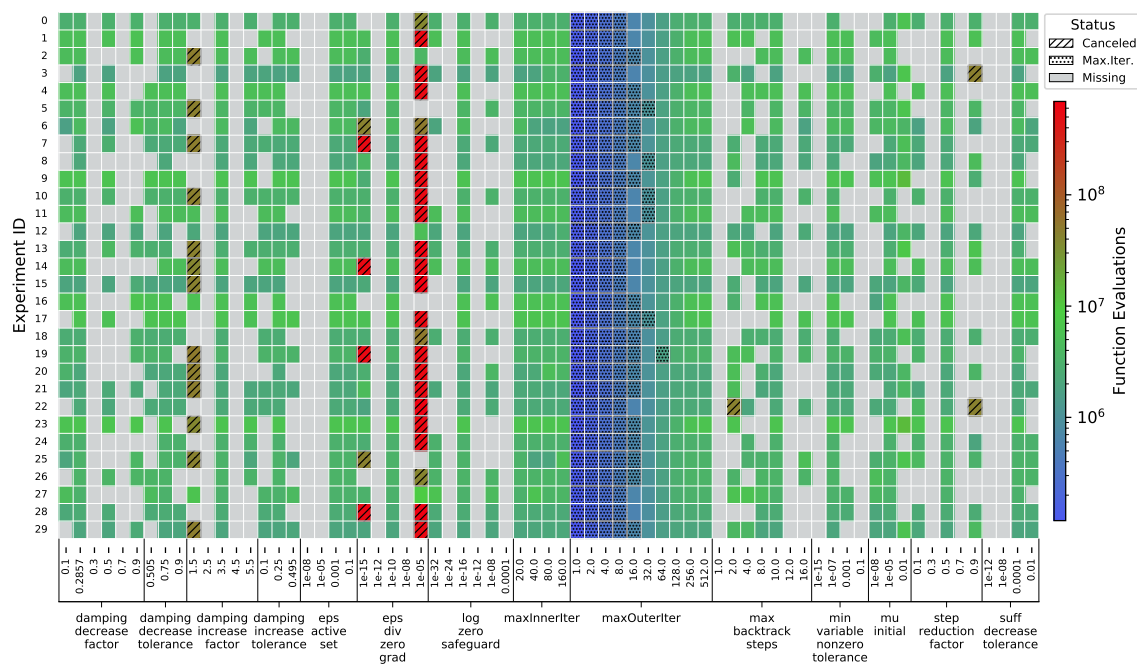


(a) PDNR, *nell-2*

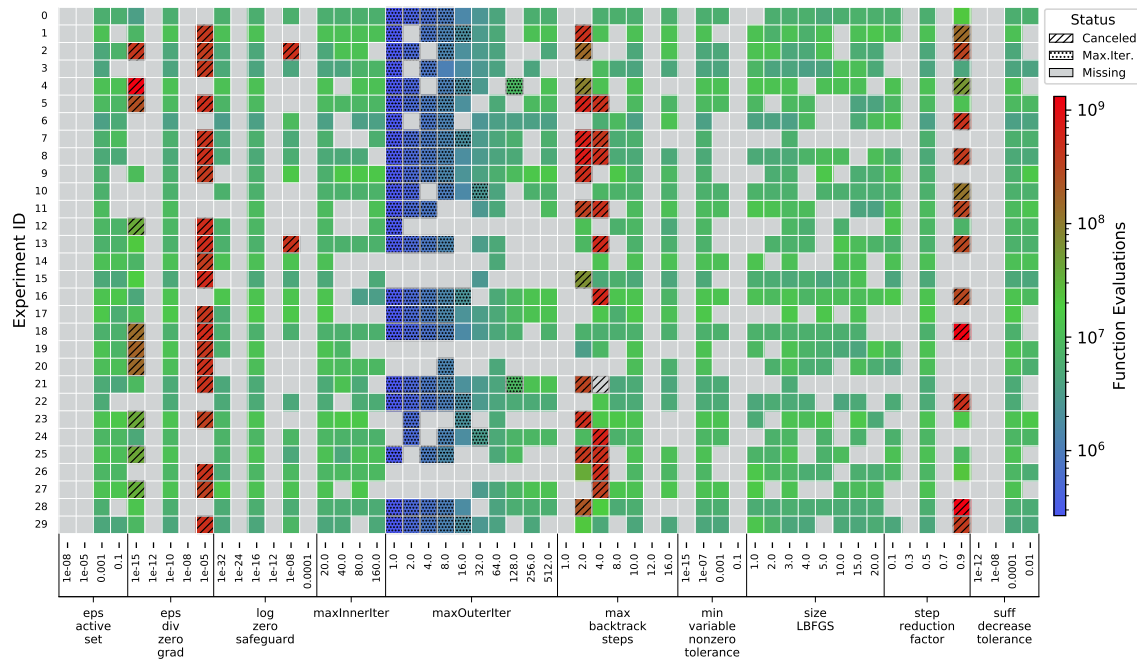


(b) PQNR, *nell-2*

Figure 11: Experiment outcomes for *chicago-crime-comm* data on IBM platform.

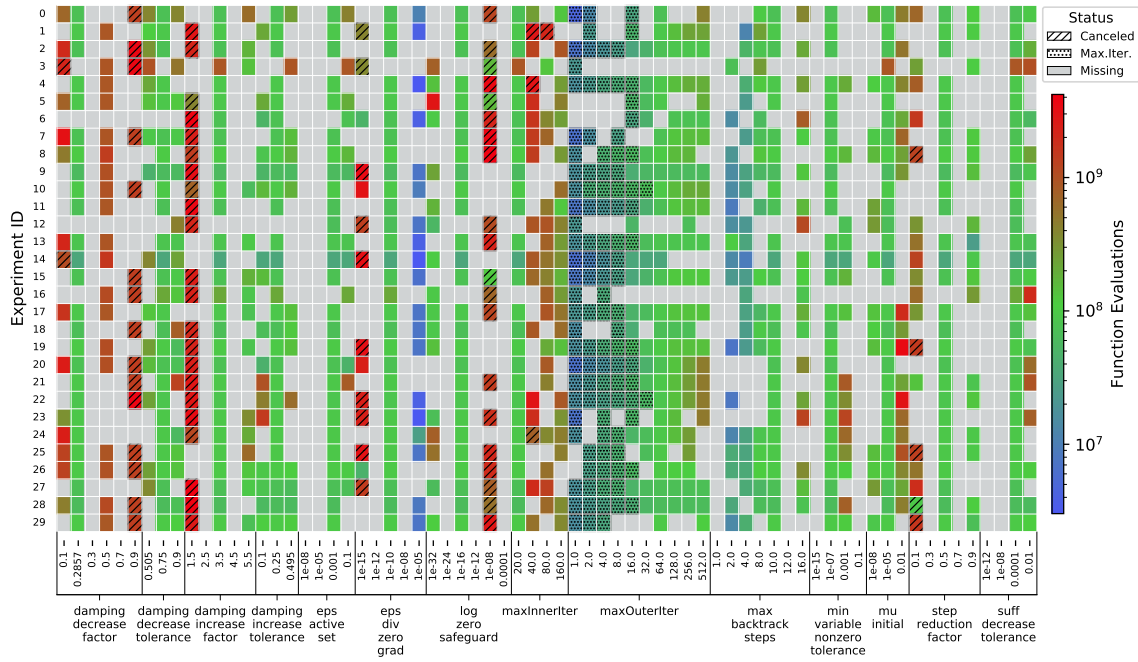


(a) PDNR, *chicago-crime-comm*

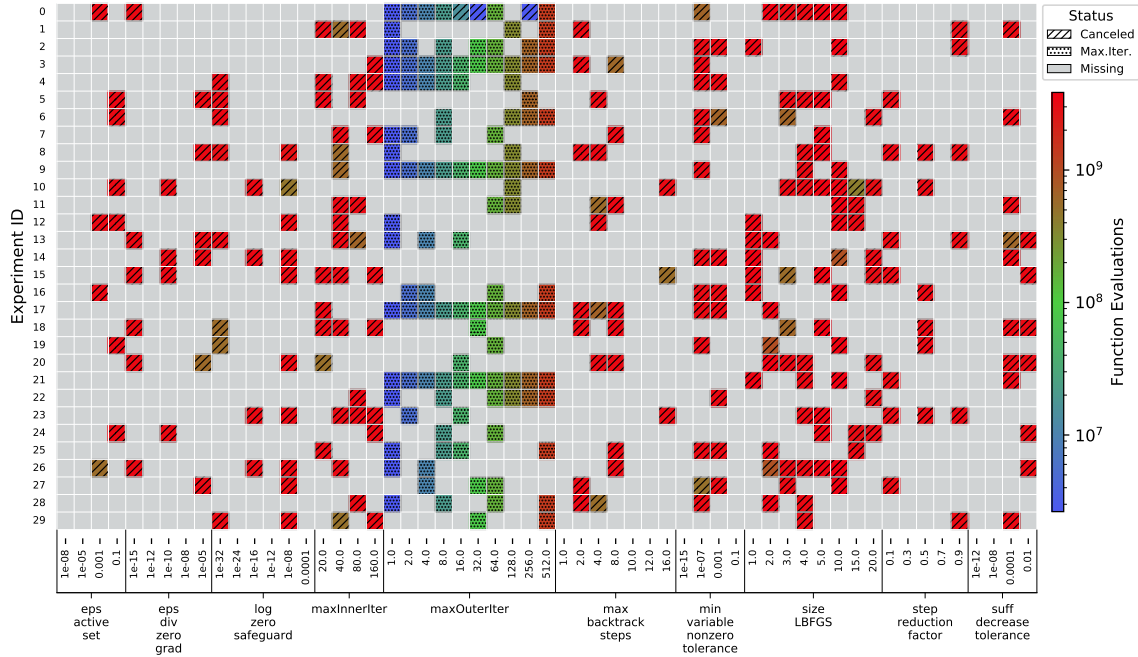


(b) PQNR, *chicago-crime-comm*

Figure 12: Experiment outcomes for *lbnl-network* data on IBM platform.

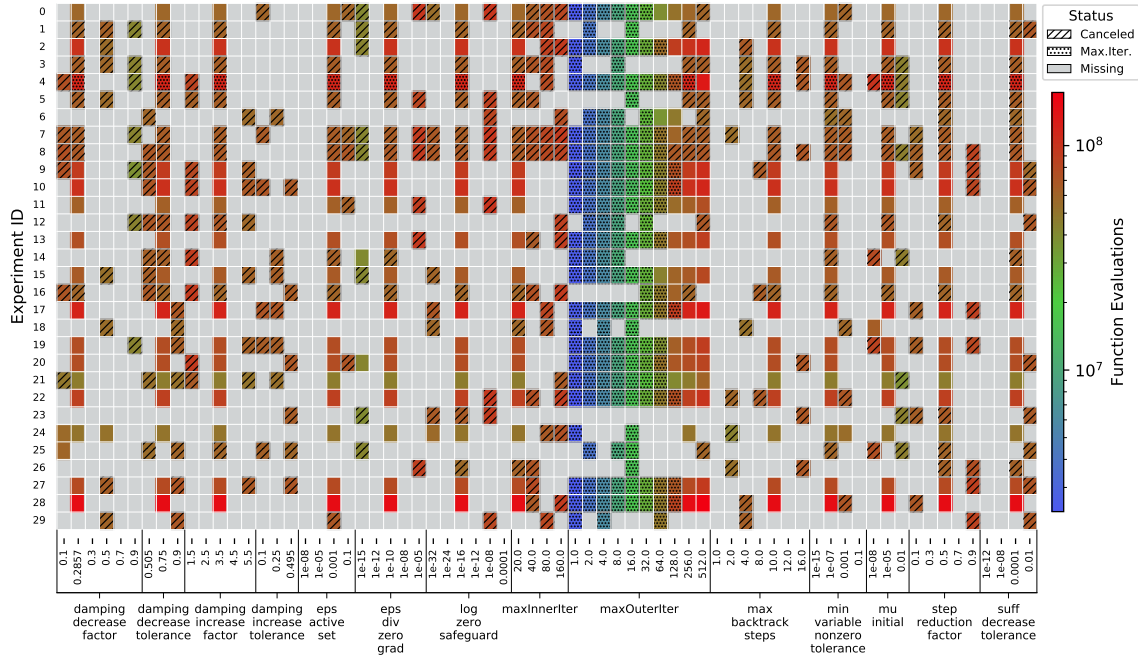


(a) PDNR, *lbnl-network*

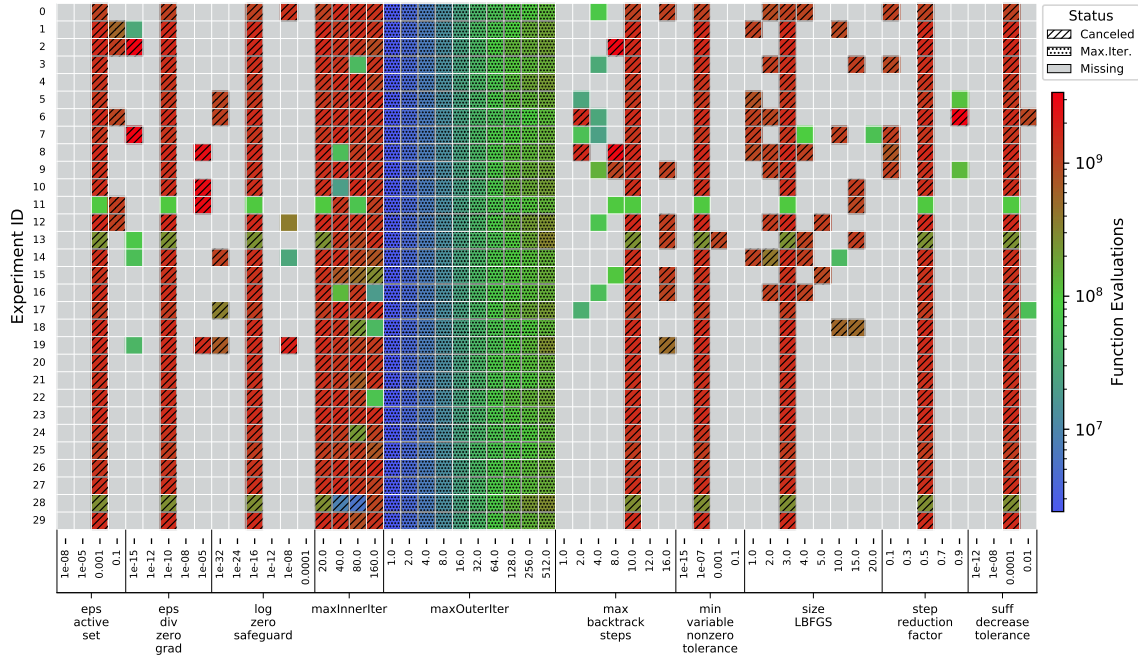


(b) PQNR, *lbnl-network*

Figure 13: Experiment outcomes for *nell-2* data on IBM platform.



(a) PDNR, *nell-2*



(b) PQNR, *nell-2*

A.2 Average Convergence Results

Below are tables presenting the number of of objective function evaluations for PDNR and PQNR to reach convergence, averaged across hardware platforms and reported per data set. N denotes number of *converged* experiments per set of experiments. Mean and 95% confidence intervals (CI) are given for objection function evaluation results.

Table 5: Average convergence behavior for the *chicago-crime-comm* data set. Confidence intervals are percentages of the mean.

Parameter	Value	Solver	N	Function Evaluations		Parameter	Value	Solver	N	Function Evaluations		
				Mean	95% CI					Mean	95% CI	
μ_{initial}	1e-08	PDNR	78	3.30e+06	± 8.2	$\text{max_outer_iterations}$	8	PQNR	3	1.03e+06	± 26.9	
	1e-05	PDNR	90	3.54e+06	± 7.9		16	PDNR	36	6.43e+05	± 1.4	
	0.01	PDNR	76	6.80e+06	± 10.2			PQNR	48	1.94e+06	± 3.9	
damping_decrease_factor	0.1	PDNR	82	3.49e+06	± 8.3		32	PDNR	75	1.03e+06	± 1.2	
	0.2857	PDNR	90	3.54e+06	± 7.9			PQNR	74	3.06e+06	± 2.5	
	0.3	PDNR	27	3.49e+06	± 16.9		64	PDNR	87	1.69e+06	± 1.0	
	0.5	PDNR	79	3.55e+06	± 8.8			PQNR	83	4.66e+06	± 2.7	
	0.7	PDNR	26	3.80e+06	± 15.4		128	PDNR	90	2.69e+06	± 3.3	
	0.9	PDNR	77	4.02e+06	± 8.1			PQNR	66	6.93e+06	± 5.8	
damping_decrease_tolerance	0.505	PDNR	77	3.56e+06	± 8.6		256	PDNR	90	3.48e+06	± 7.5	
	0.75	PDNR	90	3.54e+06	± 7.9			PQNR	73	8.50e+06	± 9.0	
	0.9	PDNR	82	3.45e+06	± 8.6		512	PDNR	90	3.54e+06	± 7.9	
damping_increase_factor	1.5	PDNR	31	3.97e+06	± 13.8		PQNR	77	8.51e+06	± 8.6		
	2.5	PDNR	30	3.53e+06	± 14.8	1	PDNR	29	3.64e+06	± 12.6		
	3.5	PDNR	90	3.54e+06	± 7.9		PQNR	7	1.52e+07	± 46.4		
	4.5	PDNR	30	3.45e+06	± 14.7	2	PDNR	75	3.87e+06	± 7.5		
	5.5	PDNR	80	3.42e+06	± 9.1		PQNR	14	1.69e+07	± 40.9		
damping_increase_tolerance	0.1	PDNR	78	3.46e+06	± 8.5	4	PDNR	77	3.85e+06	± 7.6		
	0.25	PDNR	90	3.54e+06	± 7.9		PQNR	29	1.04e+07	± 23.0		
	0.495	PDNR	76	3.47e+06	± 9.0	8	PDNR	80	3.51e+06	± 8.4		
eps_active_set	1e-08	PDNR	30	3.53e+06	± 14.3	$\text{max_backtrack_steps}$	PQNR	30	8.73e+06	± 14.5		
		PDNR	30	3.53e+06	± 14.3		10	PDNR	90	3.54e+06	± 7.9	
	1e-05	PQNR	30	8.28e+06	± 14.5			PQNR	88	8.37e+06	± 8.0	
		PDNR	90	3.54e+06	± 7.9		12	PDNR	30	3.51e+06	± 15.8	
	0.001	PQNR	88	8.37e+06	± 8.0			PQNR	29	8.08e+06	± 12.0	
		PDNR	90	3.54e+06	± 7.9		16	PDNR	75	3.57e+06	± 9.1	
	0.1	PQNR	53	8.16e+06	± 10.6			PQNR	54	8.44e+06	± 10.5	
		PDNR	67	3.20e+06	± 9.3		1e-15	PDNR	30	3.54e+06	± 14.2	
	eps_div_zero_grad	1e-15	PQNR	20	1.14e+07		± 24.0		PQNR	30	8.73e+06	± 14.5
			PDNR	30	3.59e+06		± 13.5	1e-07	PDNR	90	3.54e+06	± 7.9
		1e-12	PQNR	25	8.28e+06		± 15.3		PQNR	88	8.37e+06	± 8.0
			PDNR	90	3.54e+06		± 7.9	0.001	PDNR	80	3.56e+06	± 8.5
1e-10		PQNR	88	8.37e+06	± 8.0		PQNR	47	8.26e+06	± 11.1		
		PDNR	30	4.57e+06	± 14.9	0.1	PDNR	30	3.54e+06	± 14.2		
1e-08		PQNR	30	8.45e+06	± 14.0		PQNR	30	8.46e+06	± 15.3		
		PDNR	11	5.37e+06	± 26.8	1	PQNR	51	9.30e+06	± 11.4		
log_zero_safeguard		1e-32	PDNR	76	3.52e+06	± 8.9	size_LBFGS	2	PQNR	51	7.89e+06	± 10.9
			PQNR	56	7.90e+06	± 10.6		3	PQNR	88	8.37e+06	± 8.0
		1e-24	PDNR	30	3.55e+06	± 15.1		4	PQNR	50	7.44e+06	± 10.0
			PQNR	30	8.49e+06	± 14.5		5	PQNR	49	8.14e+06	± 11.8
	1e-16	PDNR	90	3.54e+06	± 7.9	10		PQNR	47	7.26e+06	± 11.2	
		PQNR	88	8.37e+06	± 8.0	10		PQNR	55	8.12e+06	± 10.2	
	1e-12	PDNR	30	3.45e+06	± 15.3	20		PQNR	49	7.23e+06	± 11.8	
		PQNR	30	8.01e+06	± 15.0	0.1		PDNR	79	3.61e+06	± 8.2	
	1e-08	PDNR	78	3.46e+06	± 8.5			PQNR	51	8.42e+06	± 10.6	
		PQNR	47	8.81e+06	± 11.2	0.3		PDNR	30	3.59e+06	± 13.4	
	0.0001	PQNR	8	6.48e+07	± 73.8			PQNR	30	8.11e+06	± 15.4	
		PDNR	90	3.54e+06	± 7.9	0.5		PDNR	90	3.54e+06	± 7.9	
max_inner_iterations	20	PQNR	88	8.37e+06	± 8.0		PQNR	88	8.37e+06	± 8.0		
		PDNR	90	3.51e+06	± 8.7	0.7	PDNR	30	3.88e+06	± 14.6		
	40	PQNR	49	8.42e+06	± 11.7		PQNR	26	7.97e+06	± 18.3		
		PDNR	90	3.59e+06	± 8.1	0.9	PDNR	71	3.96e+06	± 8.4		
	80	PQNR	52	8.68e+06	± 11.3		PQNR	12	1.20e+07	± 29.8		
		PDNR	90	3.68e+06	± 7.6	1e-12	PDNR	30	3.52e+06	± 14.6		
	160	PQNR	52	8.26e+06	± 10.8		PQNR	30	8.19e+06	± 14.5		
		PDNR	90	3.68e+06	± 7.6	1e-08	PDNR	30	3.52e+06	± 14.6		
		PQNR	52	8.26e+06	± 10.8		PQNR	30	8.13e+06	± 14.7		
		PDNR	90	3.54e+06	± 7.9	0.0001	PDNR	90	3.54e+06	± 7.9		
		PQNR	52	8.26e+06	± 10.8		PQNR	88	8.37e+06	± 8.0		
		PDNR	78	3.50e+06	± 8.7	0.01	PDNR	78	3.50e+06	± 8.7		
						PQNR	51	8.38e+06	± 10.9			

Table 6: Average convergence behavior for the *lbnl-network* data set. Confidence intervals are percentages of the mean.

Parameter	Value	Solver	N	Function Evaluations Mean	95% CI	Parameter	Value	Solver	N	Function Evaluations Mean	95% CI
mu_initial	1e-08	PDNR	74	1.84e+08	± 23.0	max_inner_iterations	20	PDNR	88	2.36e+08	± 25.1
	1e-05	PDNR	89	2.34e+08	± 25.1		40	PDNR	69	1.13e+09	± 13.6
	0.01	PDNR	78	7.83e+08	± 23.9		80	PDNR	77	7.31e+08	± 13.9
damping_decrease_factor	0.1	PDNR	71	1.56e+09	± 14.4	max_outer_iterations	16	PDNR	35	4.32e+07	± 6.4
	0.2857	PDNR	86	2.30e+08	± 25.4		32	PDNR	69	5.85e+07	± 4.2
	0.3	PDNR	20	3.29e+08	± 28.6		64	PDNR	86	8.33e+07	± 3.9
	0.5	PDNR	79	1.02e+09	± 4.2		128	PDNR	82	1.21e+08	± 6.5
damping_decrease_tolerance	0.505	PDNR	75	2.70e+08	± 21.3	256	PDNR	83	1.62e+08	± 10.4	
	0.75	PDNR	87	2.30e+08	± 25.2	512	PDNR	81	2.20e+08	± 16.1	
	0.9	PDNR	79	2.63e+08	± 25.4	max_backtrack_steps	1	PDNR	25	1.05e+08	± 15.7
damping_increase_factor	2.5	PDNR	30	1.58e+08	± 32.1		2	PDNR	77	2.85e+07	± 19.8
	3.5	PDNR	89	2.36e+08	± 24.9		4	PDNR	80	3.22e+07	± 10.6
	4.5	PDNR	30	1.85e+08	± 41.5		8	PDNR	79	1.39e+08	± 21.3
	5.5	PDNR	75	1.73e+08	± 22.1		10	PDNR	86	2.30e+08	± 25.4
damping_increase_tolerance	0.1	PDNR	77	2.60e+08	± 30.5		12	PDNR	28	3.76e+08	± 56.5
	0.25	PDNR	88	2.28e+08	± 25.1	16	PDNR	79	3.13e+08	± 23.8	
	0.495	PDNR	74	2.64e+08	± 27.9	1e-15	PDNR	30	2.88e+08	± 39.9	
eps_active_set	1e-08	PDNR	30	2.80e+08	± 39.8	1e-07	PDNR	87	2.29e+08	± 25.4	
	1e-05	PDNR	30	2.78e+08	± 39.7	0.001	PDNR	75	3.12e+08	± 23.6	
	0.001	PDNR	87	2.28e+08	± 25.4	0.1	PDNR	25	2.66e+08	± 43.3	
	0.1	PDNR	73	2.49e+08	± 23.9	step_reduction_factor	0.1	PDNR	59	1.01e+09	± 23.4
eps_div_zero_grad	1e-15	PDNR	33	1.85e+09	± 29.8		0.3	PDNR	29	3.61e+08	± 39.5
	1e-12	PDNR	29	1.38e+09	± 21.2		0.5	PDNR	87	2.29e+08	± 25.4
	1e-10	PDNR	89	2.27e+08	± 25.1		0.7	PDNR	29	7.52e+07	± 30.1
	1e-08	PDNR	30	2.45e+07	± 22.7	0.9	PDNR	77	1.65e+08	± 15.2	
	1e-05	PDNR	79	7.28e+06	± 14.3	suff_decrease_tolerance	1e-12	PDNR	30	2.98e+08	± 40.7
log_zero_safeguard	1e-32	PDNR	77	2.95e+08	± 43.7		1e-08	PDNR	30	2.91e+08	± 44.0
	1e-24	PDNR	30	2.82e+08	± 40.2		0.0001	PDNR	90	2.34e+08	± 24.8
	1e-16	PDNR	87	2.29e+08	± 25.4	0.01	PDNR	78	3.78e+08	± 29.8	
	1e-12	PDNR	30	4.20e+08	± 66.9						

Table 7: Average convergence behavior for the *nell-2* data set. Confidence intervals are percentages of the mean.

Parameter	Value	Solver	N	Function Evaluations Mean	95% CI	Parameter	Value	Solver	N	Function Evaluations Mean	95% CI
mu_initial	1e-08	PDNR	14	1.01e+08	± 19.9		20	PDNR	74	8.94e+07	± 6.8
	1e-05	PDNR	65	9.08e+07	± 7.1		PQNR	1	9.69e+07	± 0.0	
damping_decrease_factor	0.1	PDNR	20	9.74e+07	± 15.4	max_inner_iterations	40	PDNR	48	1.19e+08	± 16.5
	0.2857	PDNR	74	8.94e+07	± 6.8		PQNR	3	6.77e+07	± 199.0	
	0.3	PDNR	11	1.00e+08	± 20.3		80	PDNR	46	1.28e+08	± 13.8
	0.5	PDNR	24	9.34e+07	± 13.7		PQNR	4	6.54e+07	± 28.7	
	0.7	PDNR	16	8.62e+07	± 17.6		160	PDNR	44	1.43e+08	± 10.3
	0.9	PDNR	19	8.68e+07	± 15.9		PQNR	3	4.37e+07	± 130.9	
damping_decrease_tolerance	0.505	PDNR	18	9.41e+07	± 13.6	max_outer_iterations	64	PDNR	13	4.01e+07	± 4.4
	0.75	PDNR	64	9.06e+07	± 7.2		128	PDNR	52	6.01e+07	± 5.3
	0.9	PDNR	21	9.76e+07	± 14.5		256	PDNR	73	7.97e+07	± 7.1
damping_increase_factor	2.5	PDNR	15	9.31e+07	± 10.8		512	PDNR	73	9.33e+07	± 6.7
	3.5	PDNR	64	9.06e+07	± 7.2		1	PDNR	1	4.82e+07	± 0.0
	4.5	PDNR	17	9.49e+07	± 12.8		PQNR	16	2.98e+08	± 50.7	
	5.5	PDNR	21	9.06e+07	± 15.0		2	PDNR	17	6.68e+07	± 16.7
damping_increase_tolerance	0.1	PDNR	19	1.04e+08	± 14.1	max_backtrack_steps	2	PQNR	16	3.76e+08	± 60.8
	0.25	PDNR	49	9.29e+07	± 7.9		4	PDNR	17	8.01e+07	± 17.6
	0.49	PDNR	16	9.03e+07	± 13.2		PQNR	26	2.02e+08	± 46.2	
eps_active_set	1e-08	PDNR	20	9.18e+07	± 11.5		8	PDNR	20	8.93e+07	± 16.0
	1e-05	PDNR	20	9.55e+07	± 12.3		PQNR	5	1.20e+08	± 87.9	
	0.001	PDNR	74	8.94e+07	± 6.8		10	PDNR	74	8.94e+07	± 6.8
		PQNR	1	9.69e+07	± 0.0		PQNR	1	9.69e+07	± 0.0	
eps_div_zero_grad	0.1	PDNR	20	9.16e+07	± 11.1	min_variable_nonzero_tolerance	16	PDNR	15	2.20e+08	± 18.9
	1e-15	PDNR	17	5.37e+07	± 13.9		1e-07	PDNR	65	9.08e+07	± 7.1
		PQNR	21	1.86e+08	± 39.8		PQNR	1	9.69e+07	± 0.0	
	1e-12	PDNR	30	6.96e+07	± 9.6		0.001	PDNR	21	9.02e+07	± 12.0
		PQNR	9	1.24e+08	± 40.1		3	PQNR	1	9.69e+07	± 0.0
	1e-10	PDNR	74	8.94e+07	± 6.8		4	PQNR	1	9.12e+07	± 0.0
log_zero_safeguard		PQNR	1	9.69e+07	± 0.0	size_LBFGS	5	PQNR	1	1.73e+08	± 0.0
	1e-32	PDNR	20	9.94e+07	± 14.8		10	PQNR	1	4.68e+07	± 0.0
	1e-24	PDNR	16	9.55e+07	± 12.5		15	PQNR	1	1.41e+08	± 0.0
		PDNR	74	8.94e+07	± 6.8		20	PQNR	2	6.06e+07	± 27.1
		PQNR	1	9.69e+07	± 0.0		0.1	PDNR	27	1.53e+08	± 17.4
	1e-12	PDNR	19	1.07e+08	± 16.1		0.5	PDNR	65	9.08e+07	± 7.1
	PQNR	1	9.56e+07	± 0.0	PQNR	1	9.69e+07	± 0.0			
suff_decrease_tolerance	1e-08	PQNR	14	2.62e+08	± 30.4	step_reduction_factor	0.7	PDNR	3	6.41e+07	± 30.5
	0.0001	PQNR	21	3.03e+08	± 37.1		PQNR	13	2.21e+08	± 45.3	
							0.9	PDNR	14	1.31e+08	± 16.8
							PQNR	17	3.77e+08	± 46.9	
							0.0001	PDNR	65	9.08e+07	± 7.1
					PQNR	1	9.69e+07	± 0.0			
					0.01	PDNR	20	9.35e+07	± 11.7		
					PQNR	2	3.75e+07	± 666.2			